Some Control Aspects of Single-Phase Power Converters with An Active Pulsating Power Buffer

YUAN Huawei
Research Fellow
Nanyang Technological University

Sep. 20, 2022

Outline

- Background of Single-Phase Converters with an APPB*
- Review of Existing Control Methods
- Feedback-Linearization-Based APD* Control
- Lyapunov-Based APD Control
- Sensor Count Reduction Using Algebraic Observers
- Sensor Count Reduction with Simplified Algebraic Observers
- Conclusions

(1) APPB: active pulsating power buffer; (2) APD: automatic power decoupling

Single-Phase Power Converters

Function

AC-DC or DC-AC power conversion

Low power applications

- Power adaptor;
- LED driver;
- etc.

Medium power applications

- Solar micro-inverter;
- Electric vehicle charger;
- etc.

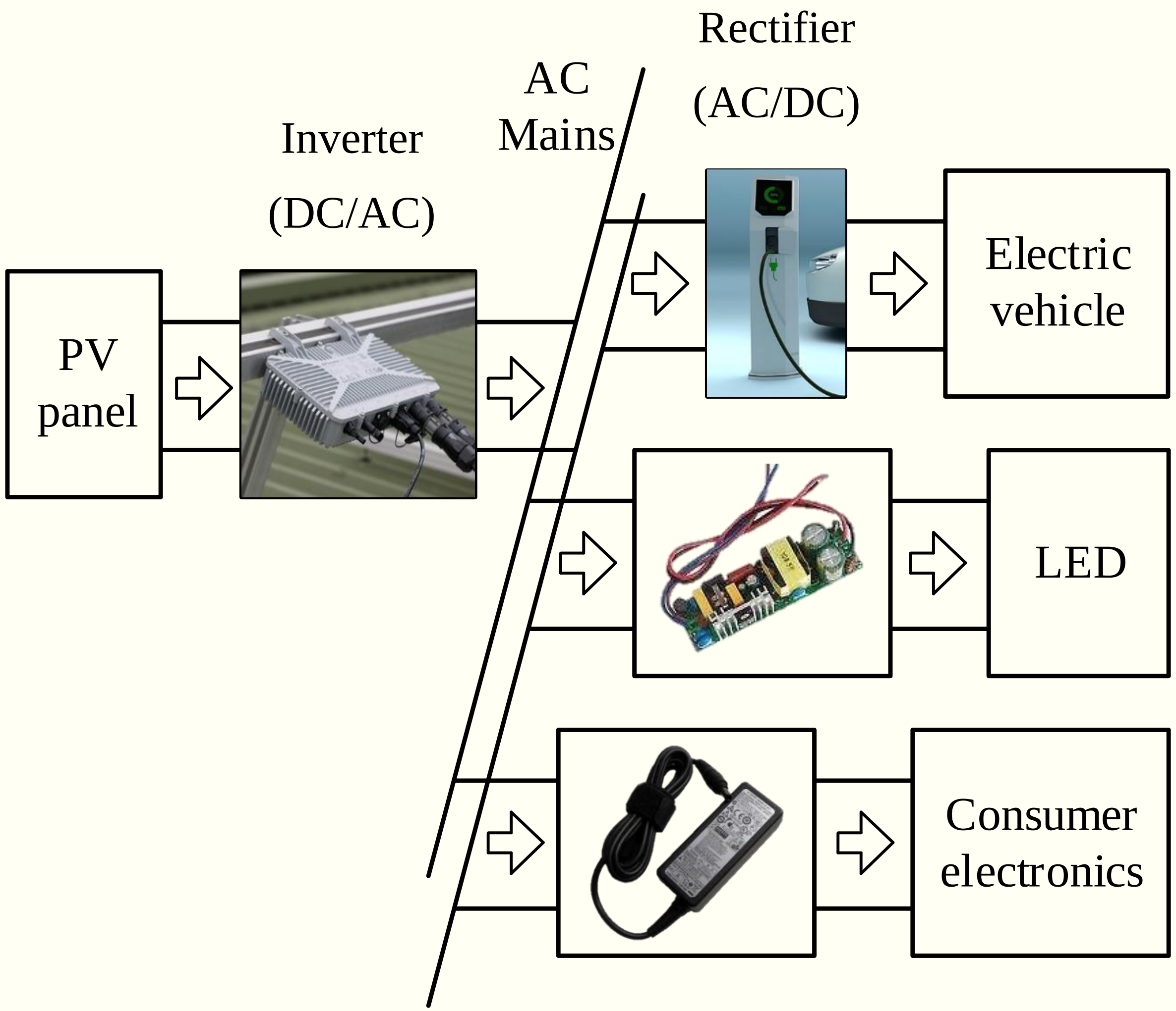

Power Imbalance Issue and Conventional Solution

Conventional converter

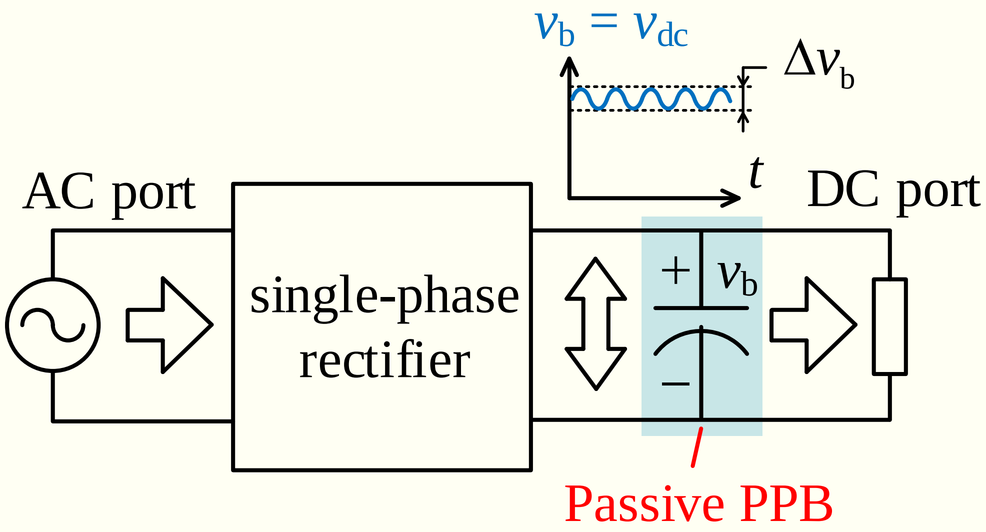

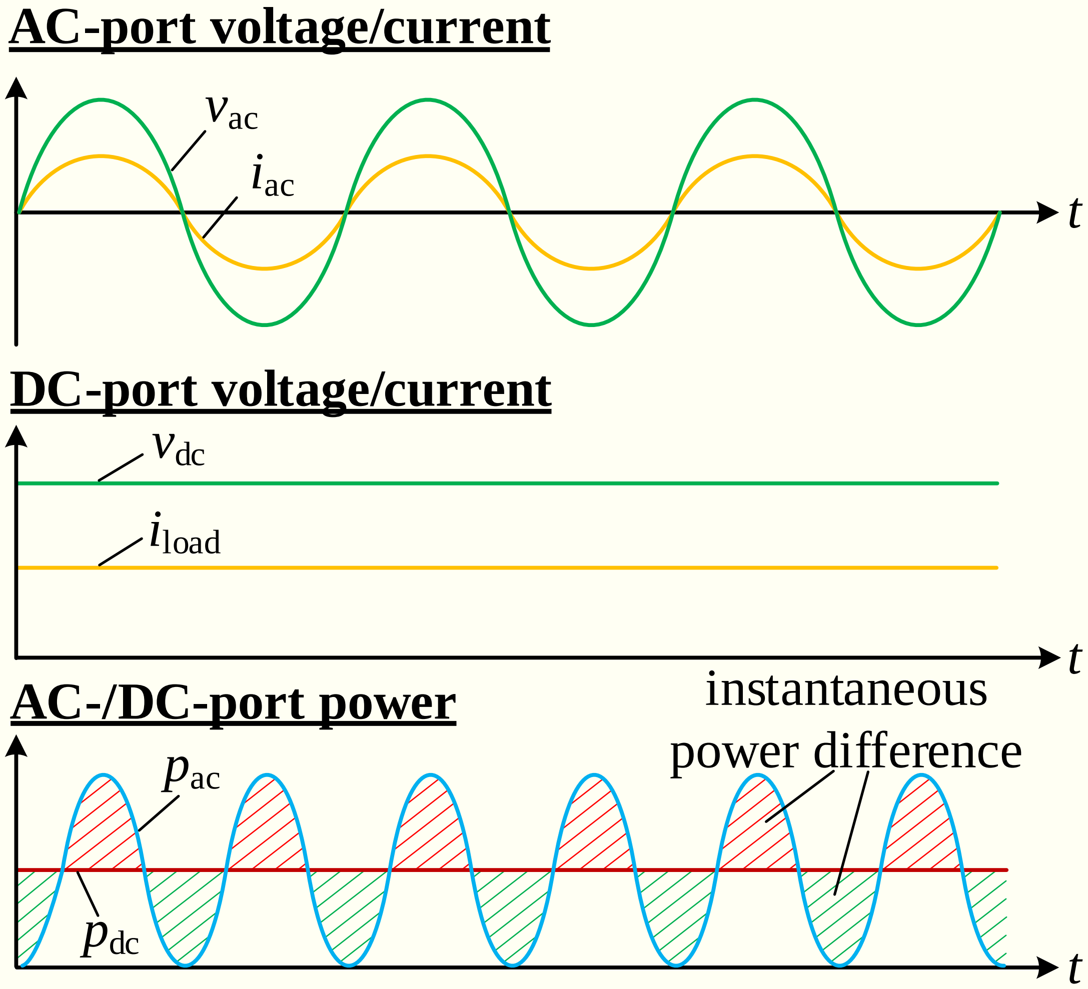

Limitations of Passive PPB Solution

- Big volume[1];
- Electrolytic capacitors (E-caps) with a short lifetime[2].

[1] R. Wang, F. Wang, D. Boroyevich, and P. Ning, "A high power density single phase PWM rectifier with active ripple energy storage," *in Proc. IEEE APEC*, Palm Springs, CA, 2010, pp. 1378–1383.

[2] L. Han, and N. Narendran, "An accelerated test method for predicting the useful life of an LED driver," *IEEE Trans. Power Electron.*, 26(8), pp. 2249–2257, Aug. 2011.

Single-Phase Converter with an APPB

APPB Solution

- A 3rd port for double-line-frequency power buffering;
- Larger allowable voltage fluctuation;
- Largely reduce capacitance requirement;
- E-cap-free design.

Advantages of APPB Solution

- Improved power density[3],[4];
- Improved reliability[5].

Converter with an APPB

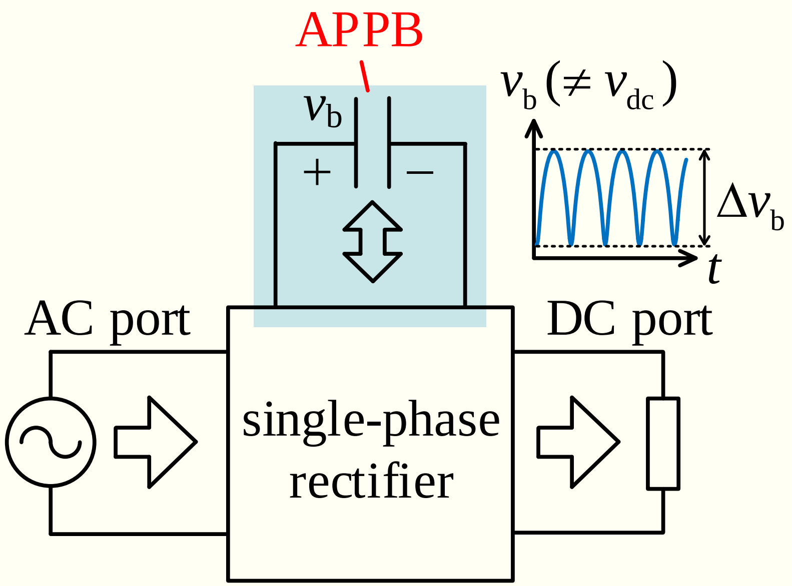

[3] D. Bortis, D. Neumayr, and J. W. Kolar, "$\eta\rho$-Pareto optimization and comparative evaluation of inverter concepts considered for the GOOGLE Little Box Challenge," *IEEE 17th COMPEL*, Trondheim, 2016, pp. 1–5.
[4] Y. Lei et al., "A 2-kW single-phase seven-level flying capacitor multilevel inverter with an active energy buffer," *IEEE Trans. Power Electron.*, 32(11), pp. 8570–8581, Nov. 2017.
[5] P. T. Krein, and R. S. Balog, "Cost-effective hundred-year life for single-phase inverters and rectifiers in solar and LED lighting applications based on minimum capacitance requirements and a ripple power port," *in Proc. IEEE APEC*, Washington, DC, 2009, pp. 620–625.

Outline

- Background of Single-Phase Converters with an APPB
- Review of Existing Control Methods
- Feedback-Linearization-Based APD Control
- Lyapunov-Based APD Control
- Sensor Count Reduction Using Algebraic Observers
- Sensor Count Reduction with Simplified Algebraic Observers
- Conclusions

According to APPB Reference Generation

Open-Loop Control[6][7]

- Approach 1 - directly calculate the APPB reference

$$\frac{d}{dt}\left(\frac{1}{2}C_\mathrm{b}\left(v_\mathrm{b}^\mathrm{R}\right)^2\right) = p_\mathrm{ac} - p_\mathrm{dc} = \frac{V_\mathrm{ac}I_\mathrm{ac}}{2}\cos(2\omega t - \varphi)$$

- Approach 2 - APPB is controlled as an active power filter

KCL: $i_\mathrm{load} = i_\mathrm{o} + i_\mathrm{PPB} = i_\mathrm{o,dc} + i_\mathrm{o,ac} + i_\mathrm{PPB}$

If $i_\mathrm{PPB}^\mathrm{R} = -i_\mathrm{o,ac}$, then $i_\mathrm{load} = i_\mathrm{o,dc}$.

Closed-Loop Control[8][9]

- APPB reference is obtained from the output

$$i_\mathrm{PPB}^\mathrm{R} = G_r(s)i_\mathrm{load,ac}, \text{ or } v_\mathrm{b}^\mathrm{R} = G_r(s)v_\mathrm{dc,ac}.$$

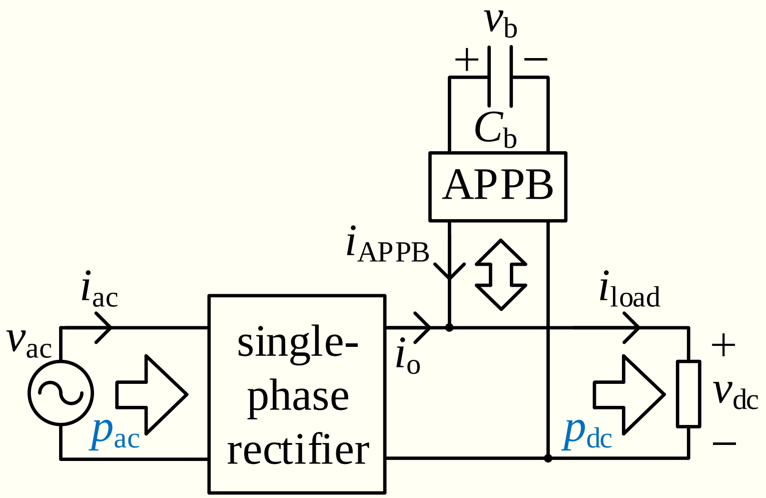

[6] S. Dusmez, and A. Khaligh, "Generalized technique of compensating low-frequency component of load current with a parallel bidirectional DC/DC converter," *IEEE Trans. Power Electron.*, vol. 29, no. 11, pp. 5892–5904, Nov. 2014.
[7] X. Huang, X. Ruan, F. Du, F. Liu, and L. Zhang, "A pulsed power supply adopting active capacitor converter for low-voltage and low-frequency pulsed loads," *IEEE Trans. Power Electron.*, vol. 33, no. 11, pp. 9219–9230, Nov. 2018.
[8] S. Li, W. Qi, S. C. Tan, and S. Y. R. Hui, "A single-stage two-switch PFC rectifier with wide output voltage range and automatic AC ripple power decoupling," *IEEE Trans. Power Electron.*, vol. 32, no. 9, pp. 6971–6982, Sept. 2017.
[9] W. Yao, X. Wang, P. C. Loh, X. Zhang, and F. Blaabjerg, "Improved power decoupling scheme for a single-phase grid-connected differential inverter with realistic mismatch in storage capacitances," *IEEE Trans. Power Electron.*, vol. 32, no. 1, pp. 186–199, Jan. 2017.

According to Control Techniques

Linear Control[10][11]

- Examples: PI control, resonance control, repetitive control, type III compensator, etc.
- **Limitations:** 1. Limited transient performance; 2. Stability may not be guaranteed during transient operation.

Nonlinear Control[12][13]

- Examples: Bang-bang control, model predictive control, partial feedback linearization, etc.
- **Limitations:** 1. Topology dependent; 2. There lacks a systematic design theory.

In This Tutorial

- To present a systematic controller design theory for this emerging class of converter.

[10] Y. Ohnuma, K. Orikawa, and J. I. Itoh, "A single-phase current-source PV inverter with power decoupling capability using an active buffer," *IEEE Trans. Ind. Appl.*, vol. 51, no. 1, pp. 531–538, Jan./Feb. 2015.
[11] W. Yao, X. Wang, P. C. Loh, X. Zhang, and F. Blaabjerg, "Improved power decoupling scheme for a single-phase grid-connected differential inverter with realistic mismatch in storage capacitances," *IEEE Trans. Power Electron.*, vol. 32, no. 1, pp. 186–199, Jan. 2017.
[12] S. Li, G. R. Zhu, S. C. Tan, and S. Y. Hui, "Direct AC/DC rectifier with mitigated low-frequency ripple through inductor-current waveform control," *IEEE Trans. Power. Electron.*, vol. 30, no. 8, pp. 4336–4348, Aug. 2015.
[13] Y. Liu, B. Ge, H. Abu-Rub, H. Sun, F. Z. Peng, and Y. Xue, "Model predictive direct power control for active power decoupled single-phase quasi-Z -source inverter," *IEEE Trans. Ind. Informat.*, vol. 12, no. 4, pp. 1550–1559, Aug. 2016.

Outline

- Background of Single-Phase Converters with an APPB
- Review of Existing Control Methods
- Feedback-Linearization-Based APD Control[14]
- Lyapunov-Based APD Control
- Sensor Count Reduction Using Algebraic Observers
- Sensor Count Reduction with Simplified Algebraic Observers
- Conclusions

[14] H. Yuan, S. Li, W. Qi, S. Tan, and S. Hui, "On nonlinear control of single-phase converters with active power decoupling function," *IEEE Trans. Power Electron.*, vol. 34, no. 6, pp. 5903–5915, June 2019.

Controller Design Considerations

Comparison of the Characteristics of the Converters

Conventional converter

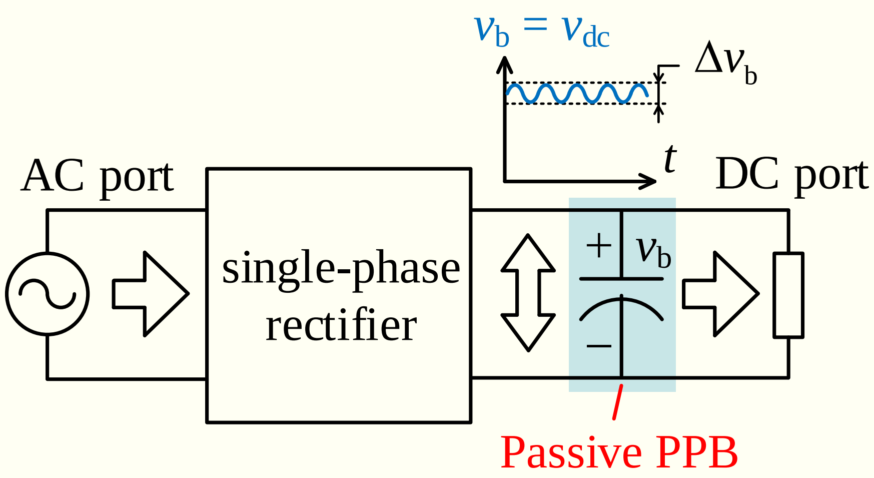

- Small signal operation
- Large dc-link inertia
- Single-input single-output controller structure

Converter with an APPB

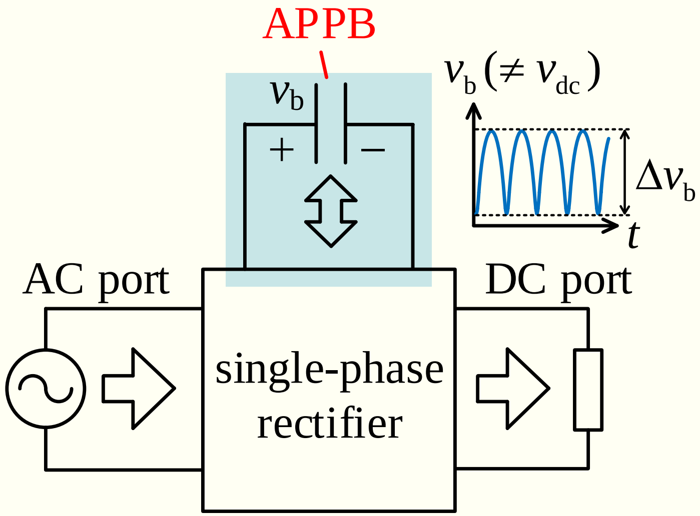

- Large signal operation
- Small dc-link inertia
- Two-input two-output controller structure

Controller Design Considerations

Three Control Strategies

- *A*: direct control of p_{ac} and p_b;
- *B*: direct control of p_{dc} and p_b;
- *C*: direct control of p_{ac} and p_{dc}.

A, *B* → Direct-power-decoupling (DPD) strategy

C → Automatic-power-decoupling (APD) strategy

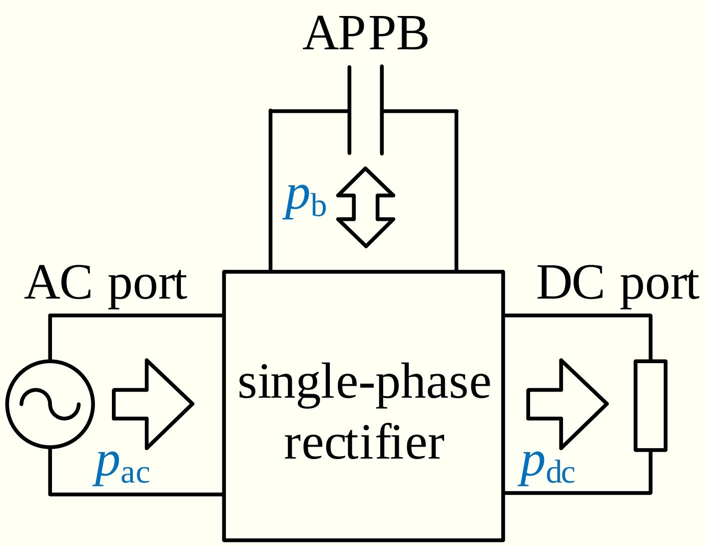

Selection of the APD Strategy

- The AC-port and DC-port references are ready to use;
- The accurate APPB reference is difficult to predict during transients.

Suggested Control Scheme

- Nonlinear control + APD strategy.

Feedback Linearization Control

Advantages

- Powerful in linearizing and decoupling a nonlinear and coupled system without approximation[15];
- Suitable for controlling the single-phase converter with an APPB.

Objectives of This Part

- To introduce a feedback-linearization-based APD (FLB-APD) control method to enhance the system performance.
- To explore some new potential of this emerging type of converter, such as reactive power compensation, harmonics compensation, and output voltage holdup.

[15] J.-J. E. Slotine, and W. Li, "Feedback Linearization" in *Applied Nonlinear Control*, 6th ed., vol. 199, no. 1, Englewood Cliffs, NJ, USA: Prentice hall, 1991, pp. 207–271.

FLB-APD Control

General Principle

- APD strategy: $y_1 = x_{ac}$; $y_2 = x_{dc}$.
- Derive the input-output model: $\mathbf{y} = \mathbf{f}(\mathbf{u}, \mathbf{x})$.
- Feedback linearization:
  1) Input transformation: $\mathbf{v} = \mathbf{K}^{-1}(\mathbf{u}, \mathbf{x})$;
  2) Equivalent system: $y_1 = G_1(s)\cdot v_1$, $y_2 = G_2(s)\cdot v_2$.
- Use simple linear control techniques to control the linearized system.

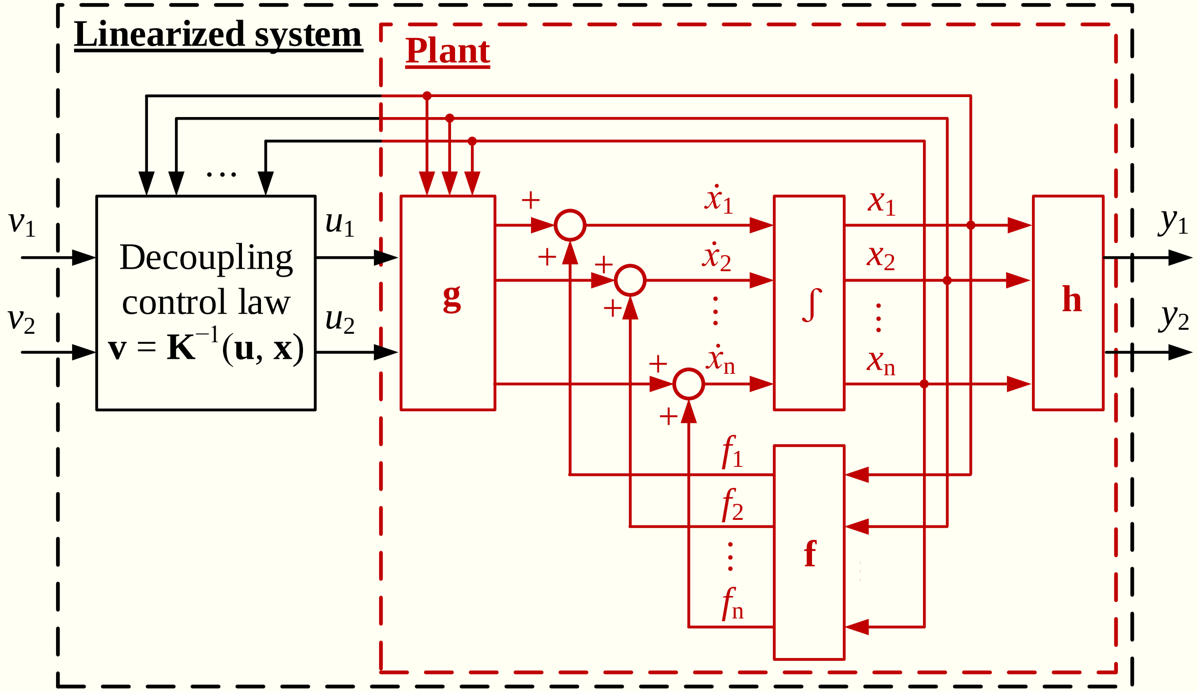

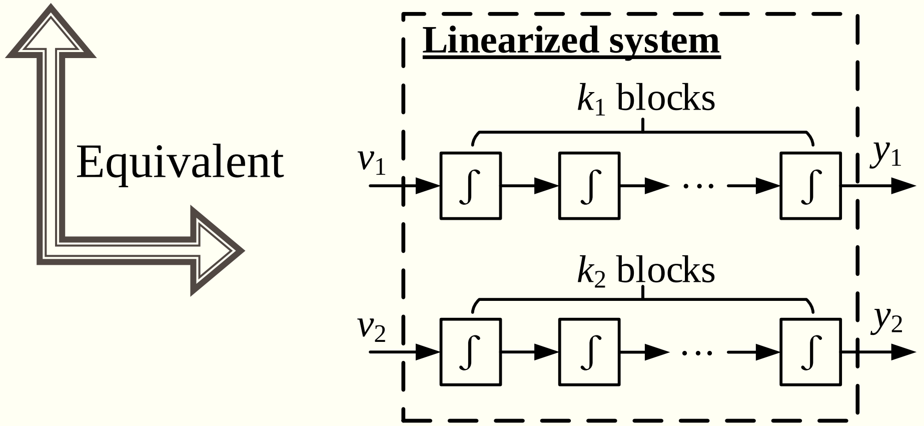

Stability of internal dynamics ($\dot{\mathbf{x}}_{\mathbf{y}} = \mathbf{d}_{\text{int}}(\mathbf{x}, \mathbf{v})$) must be checked.

FLB-APD Control

Illustration

- Structure: full-bridge rectifier + buck-type APPB (DCM* operation).
- State-space-averaged model:

$$\begin{cases} \dot{\mathbf{x}} = \mathbf{f}(\mathbf{x}) + \mathbf{g}(\mathbf{x}) \cdot \mathbf{u}, \ \ \mathbf{x} = [i_{ac}, v_{dc}, v_{b}]^{T}, \ \ \mathbf{u} = [m_{AB}, d_{C}]^{T} \\ \mathbf{y} = \mathbf{h}(\mathbf{x}) = [i_{ac}, v_{dc}]^{T}, \ \ (\overline{\mathbf{x}}_{\mathbf{y}} = \{v_{b}\}) \end{cases}$$

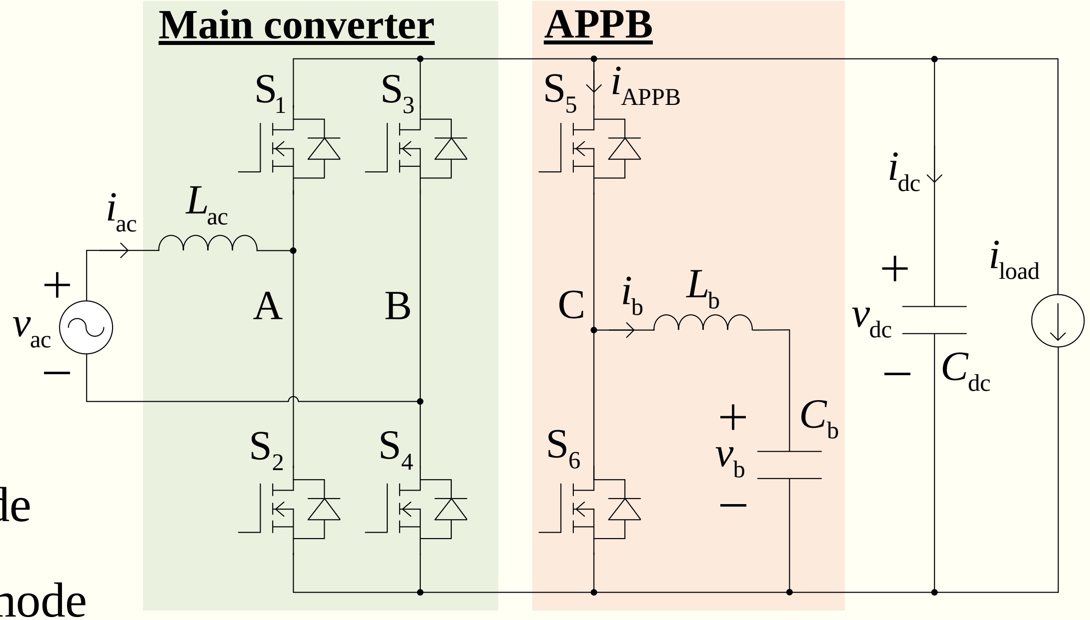

- The FLB-APD control law:

$$m_{AB} = \left(v_{ac} - L_{ac}\dot{i}_{ac}^{R} - \alpha_{1}L_{ac}(i_{ac}^{R} - i_{ac})\right) / v_{dc}$$

$$d_{C} = \begin{cases} c\left(m_{AB}i_{ac} - \alpha_{2}C_{dc}(v_{dc}^{R} - v_{dc}) - i_{load}\right) / (v_{dc} - v_{b}), \ \text{buck mode} \\ c(v_{dc} - v_{b})\left(m_{AB}i_{ac} - \alpha_{2}C_{dc}(v_{dc}^{R} - v_{dc}) - i_{load}\right) / v_{b}^{2}, \ \text{boost mode} \end{cases}$$

- Error dynamics of **y**:

$$\dot{e}_{i} + \alpha_{i}e_{i} = 0 \quad (i = 1, \ 2)$$

- Internal dynamics:

Bounded and stable v_{b}

DCM: discontinuous conduction mode.

FLB-APD Control

Illustration

- Overall control block diagram

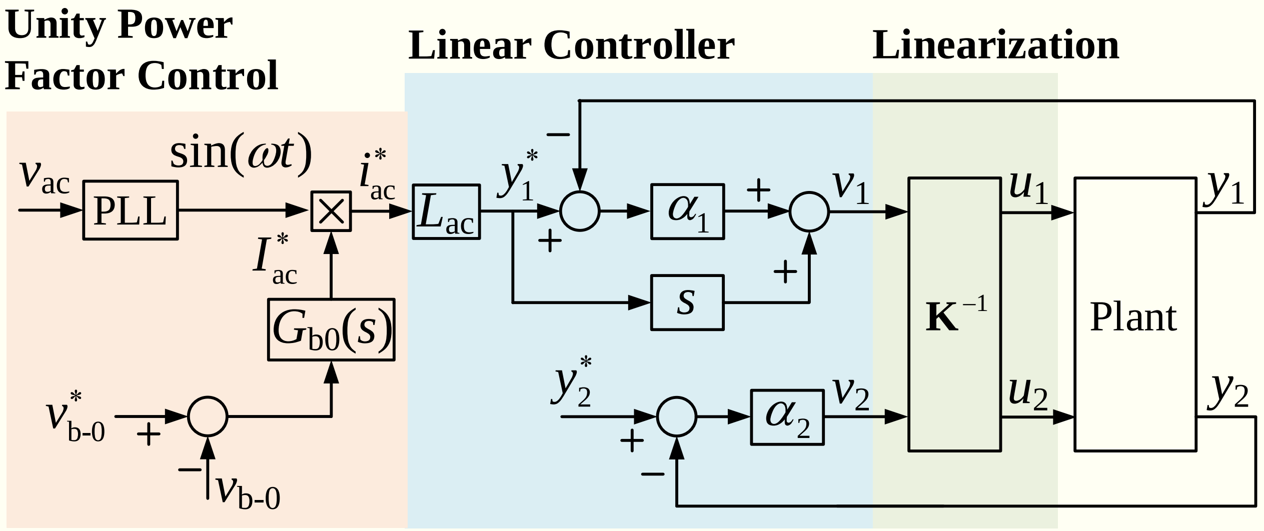

- Equivalent diagram

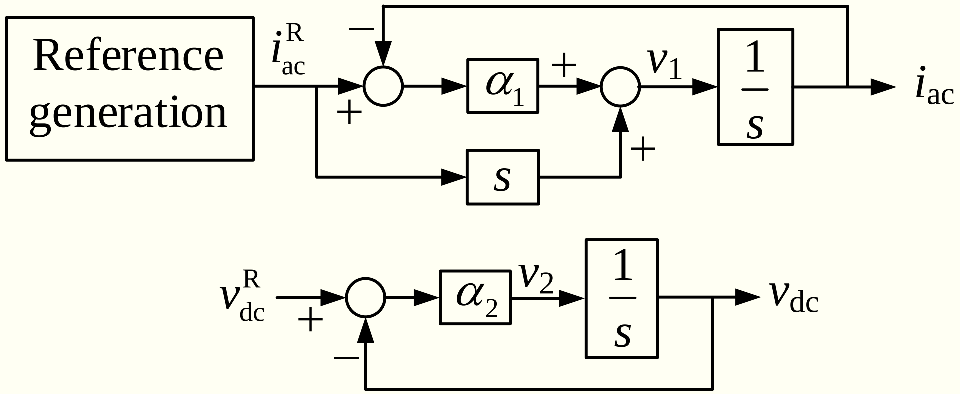

Experimental Verification

Specifications

Parameters		Values
Rated power		100 W
Switching frequency		25 kHz
AC port	v_{ac}	220 V / 50 Hz
	L_{ac}	7 mH
DC port	v_{dc}	400 V
	C_{dc}	10 μF
APPB port	C_b	30 μF
	L_b	212 μH

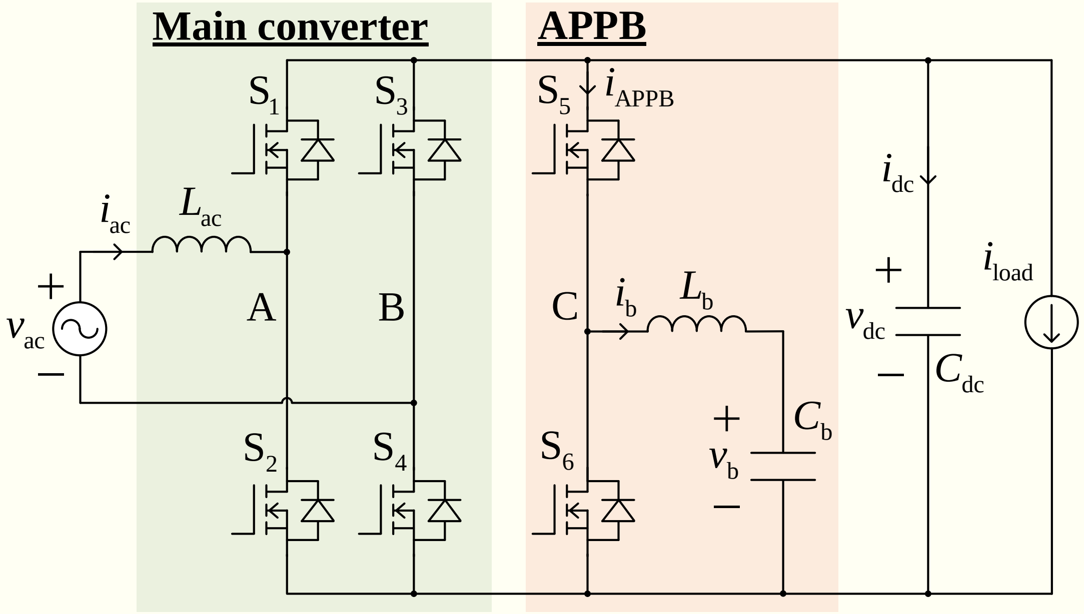

Experimental Verification

Steady-State Operation

- **AC port:**

  i) Unity power factor;

  ii) i_{ac} has a low THD* of 3.57%.

- **DC port:**

  v_{dc} tightly regulated at 400 V with a peak-to-peak ripple of 0.5%.

- **APPB port:**

  v_b has a voltage swing of 40 V. (C_b = 30 μF, while a conventional solution needs 400 μF[16].)

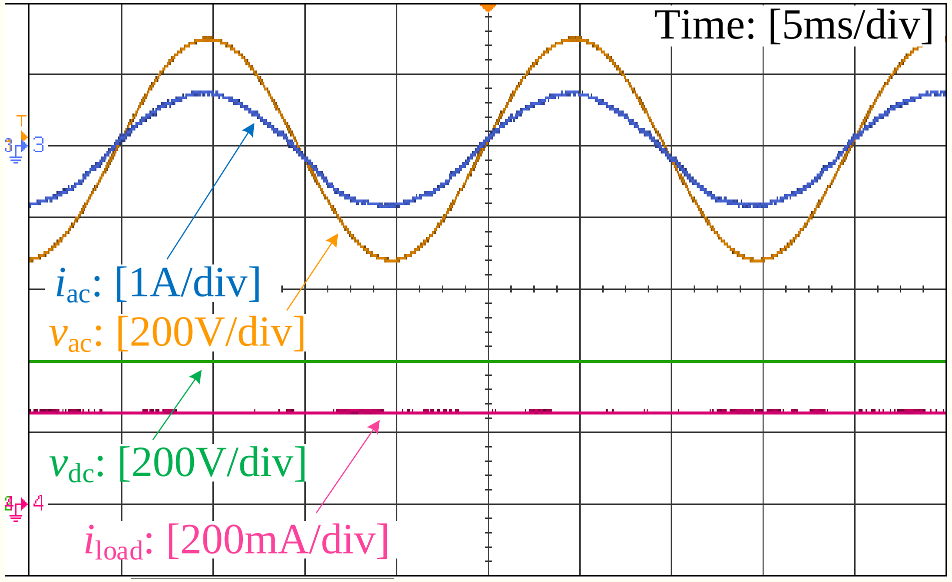

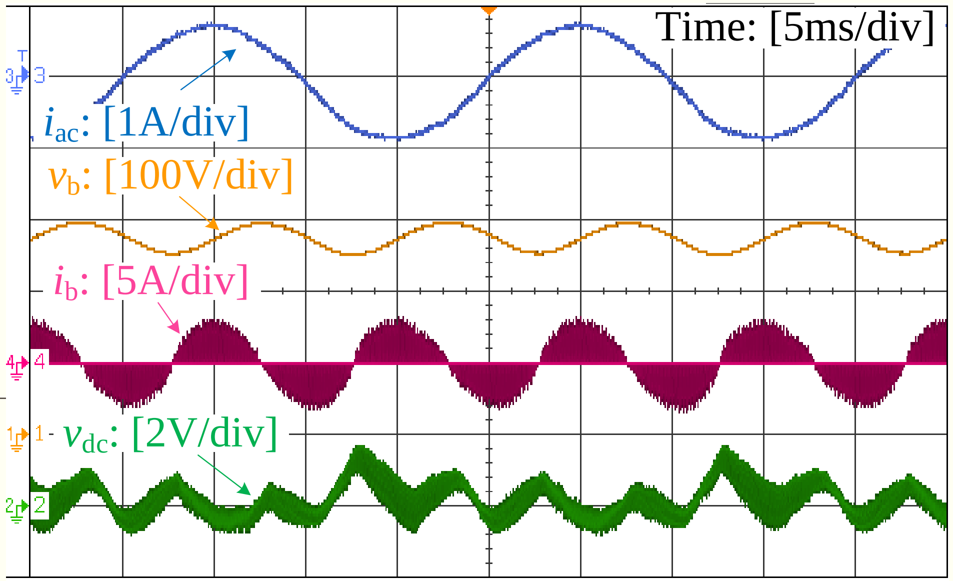

THD: total harmonic distortion.

[16] P. T. Krein, R. S. Balog, and M. Mirjafari, "Minimum energy and capacitance requirements for single-phase inverters and rectifiers using a ripple port," *IEEE Trans. Power Electron.*, 27(11), pp. 4690–4698, Nov. 2012.

Experimental Verification

Reduced APPB

- C_b reduced from 30 μF to 5.47 μF.
  (The theoretical limit of C_b: 3.98 μF[16]).
- v_b has a voltage swing of 300 V.
- The converter operates reliably.

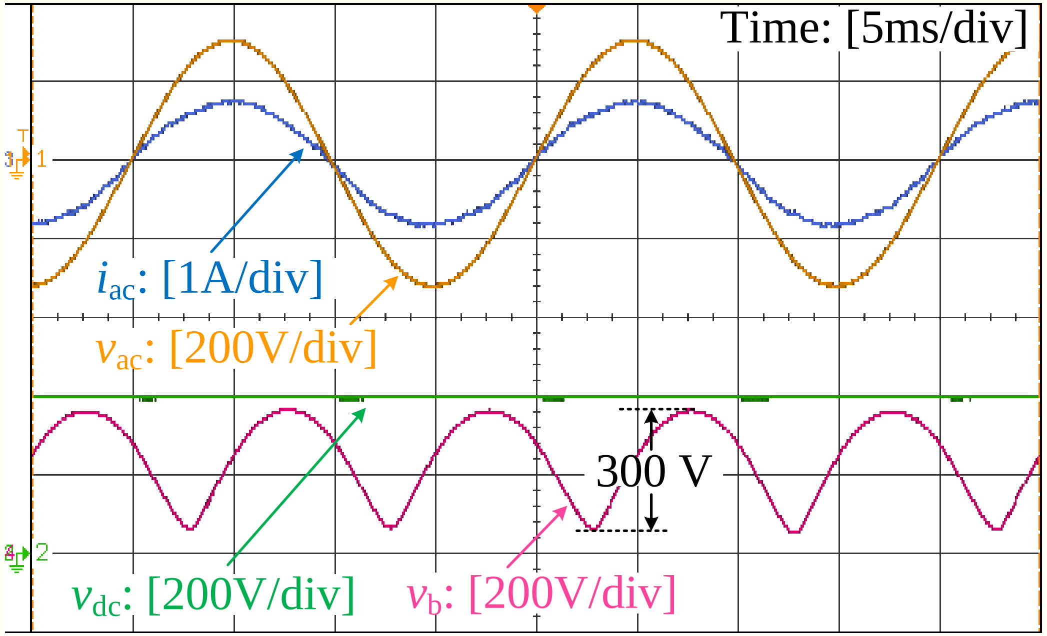

[16] P. T. Krein, R. S. Balog, and M. Mirjafari, "Minimum energy and capacitance requirements for single-phase inverters and rectifiers using a ripple port," *IEEE Trans. Power Electron.*, 27(11), pp. 4690–4698, Nov. 2012.

Experimental Verification

Load-Disturbance Test

- **Experiment condition:** Power change - 0 W → 100 W and 100 W → 0 W.
- v_{dc} remains tightly regulated.
- i_{ac} enters its steady-state within three line cycles.
- The stepped imbalanced power is buffered by the APPB (see v_b).

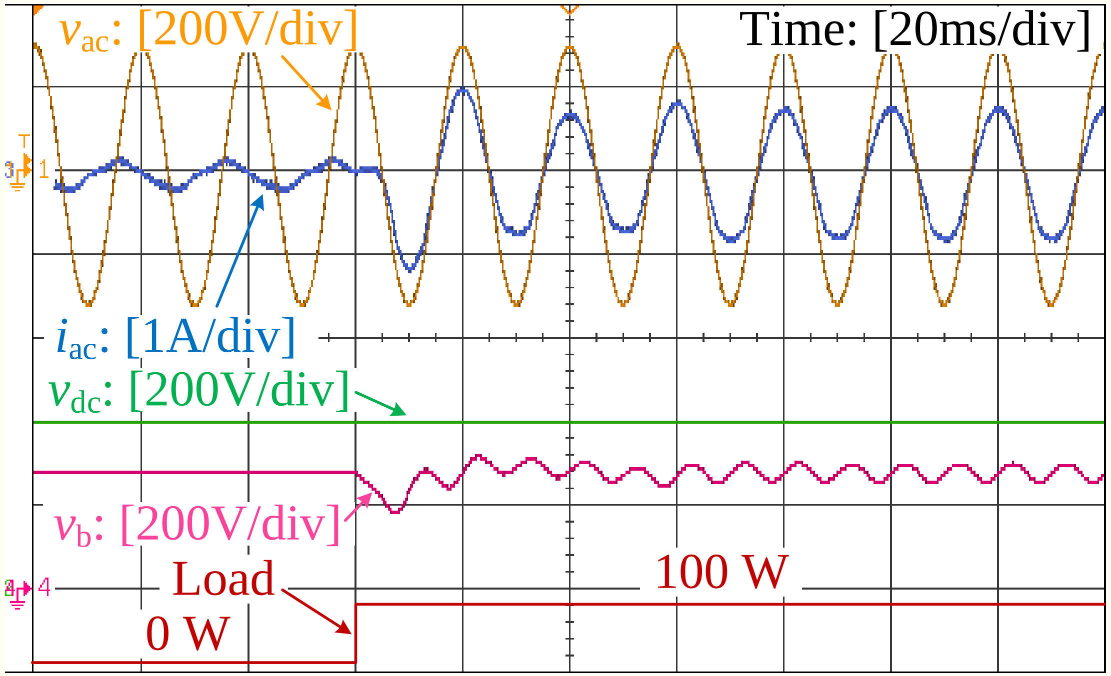

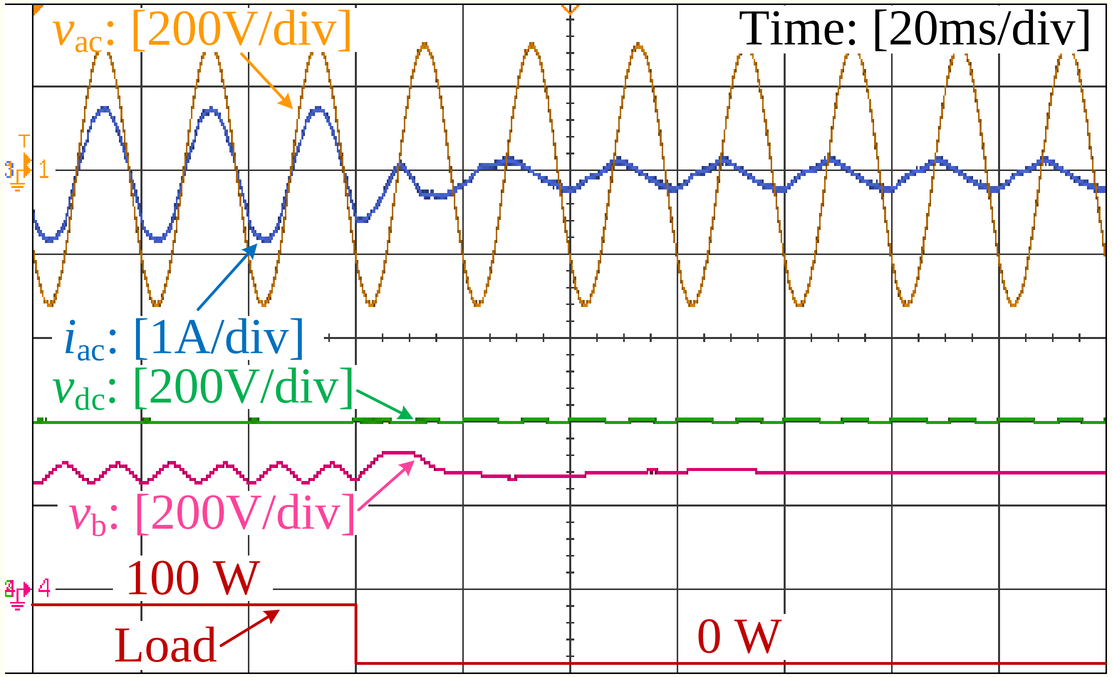

Experimental Verification

Output-Reference-Tracking Test

- **Experiment condition:**

  Reference of v_{dc}: 400 V → 450 V and 450 V → 400 V.

- v_{dc} has first-order responses with a settling time of 1 ms (designed τ_2 = 0.25 ms).

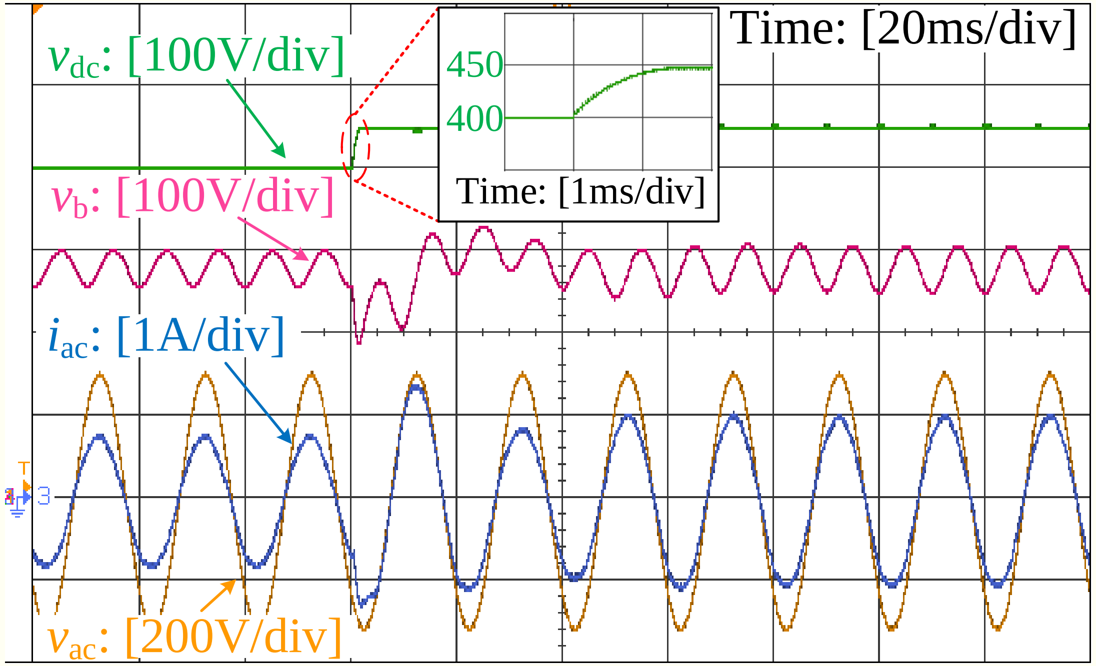

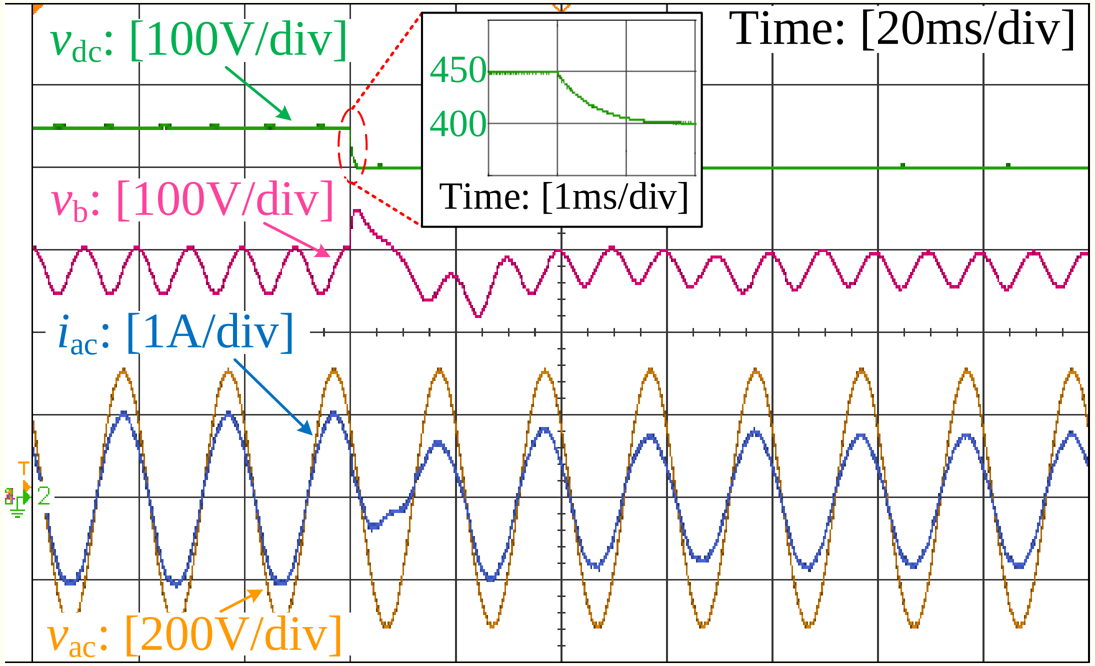

Experimental Verification

Output Voltage Holdup

- **Experiment condition:**
  The input of the converter is suddenly cut off.

- v_{dc} remains tightly regulated at 400 V for 10 ms after input shutdown.
  (Typical holdup time is half to one line cycle[17].)

- The energy stored in the APPB is fully utilized.

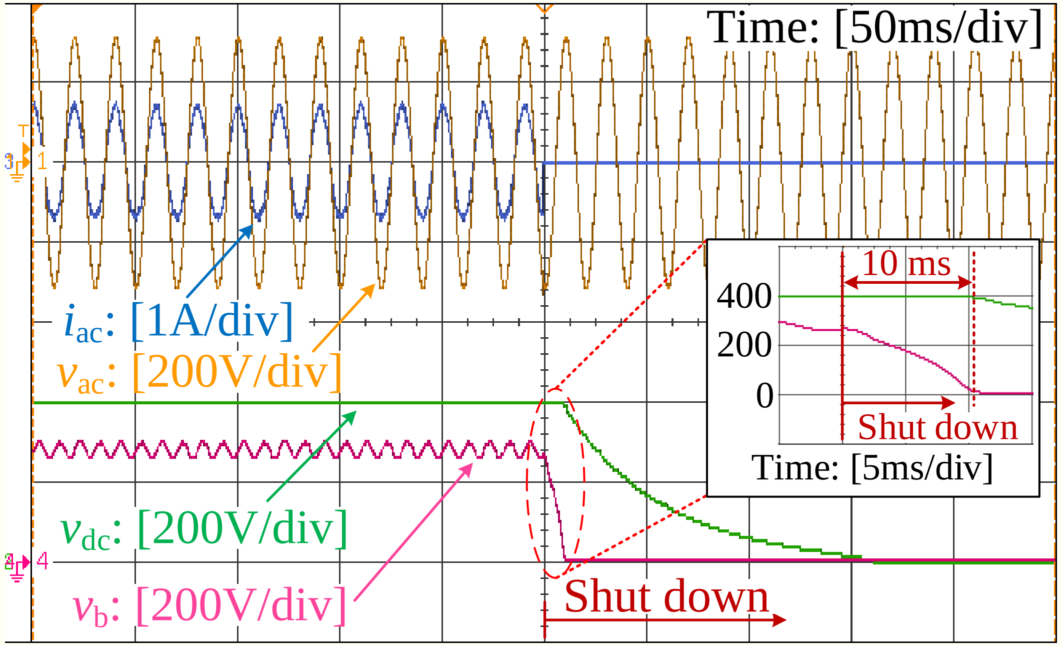

[17] Y. Jang, M.M. Jovanovic, and D.L. Dillman, "Hold-up time extension circuit with integrated magnetics," *IEEE Trans. Power Electron.*, 21(2), pp. 394–400, Mar. 2006 .

Experimental Verification

Harmonics Compensation

- **Experiment condition:** See the circuit below.
- The THD of i_g is reduced from 52.9% to 6.03%.
- v_{dc} remains tightly regulated.

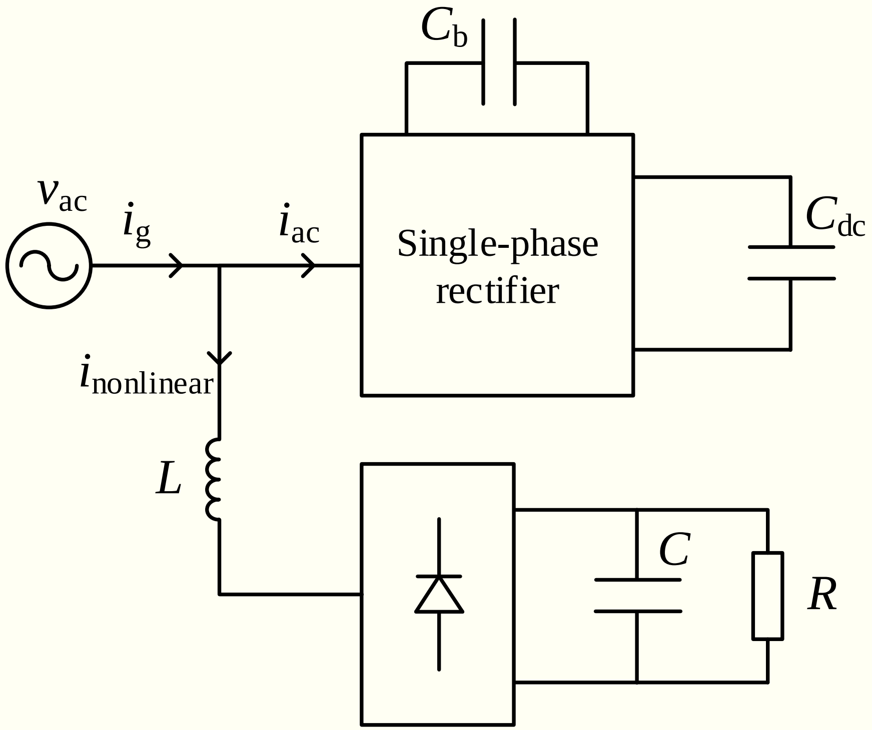

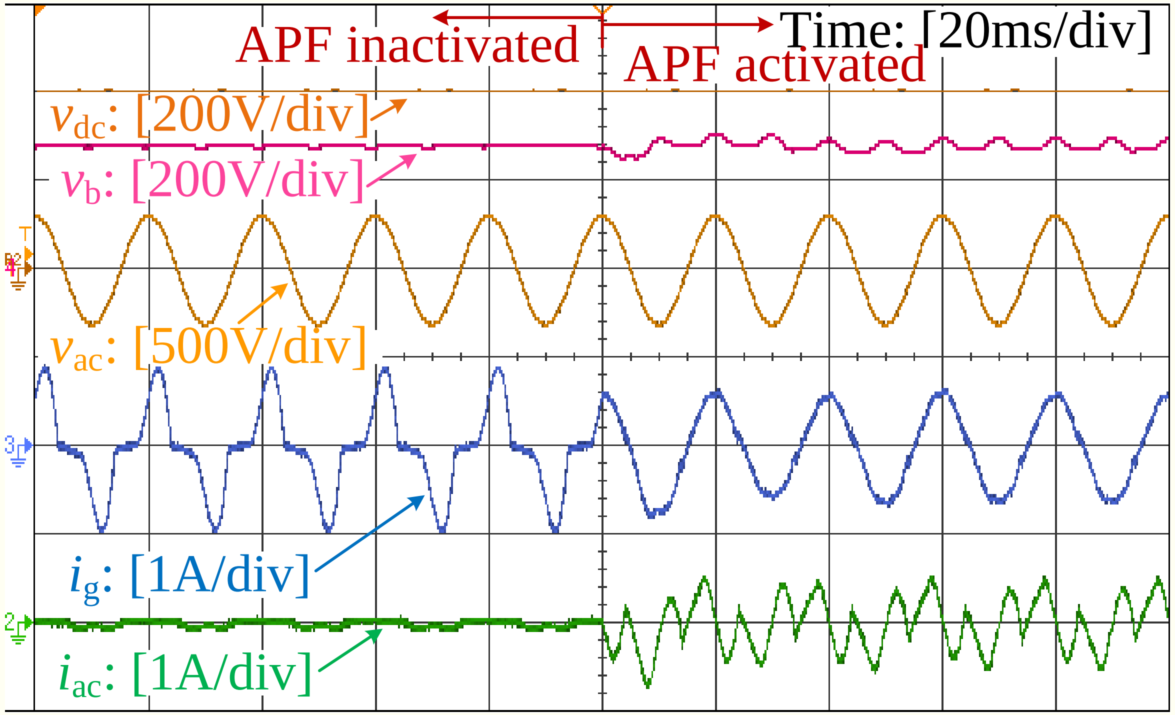

Outline

- Background of Single-Phase Converters with an APPB
- Review of Existing Control Methods
- Feedback-Linearization-Based APD Control
- Lyapunov-Based APD Control[18]
- Sensor Count Reduction Using Algebraic Observers
- Sensor Count Reduction with Simplified Algebraic Observers
- Conclusions

[18] H. Yuan, S. Li, S. Tan, and S. Y. R. Hui, “Internal dynamics stabilization of single-phase power converters with Lyapunov-based automatic-power-decoupling control,” *IEEE Trans. Power Electron.*, vol. 35, no. 2, pp. 2160–2169, Feb. 2020.

Introduction

Limitation of FLB-APD Control

- Unable to ensure the stability of internal dynamics for some systems.

Objectives of This Part

- To explain the instability issue of using the FLB-APD control with an example circuit;
- To stabilize the internal dynamics using the LB-APD control.

Mathematical Modeling

Example Circuit

- Topology: full-bridge rectifier + buck-type APPB.
- The APPB operates in the CCM*.

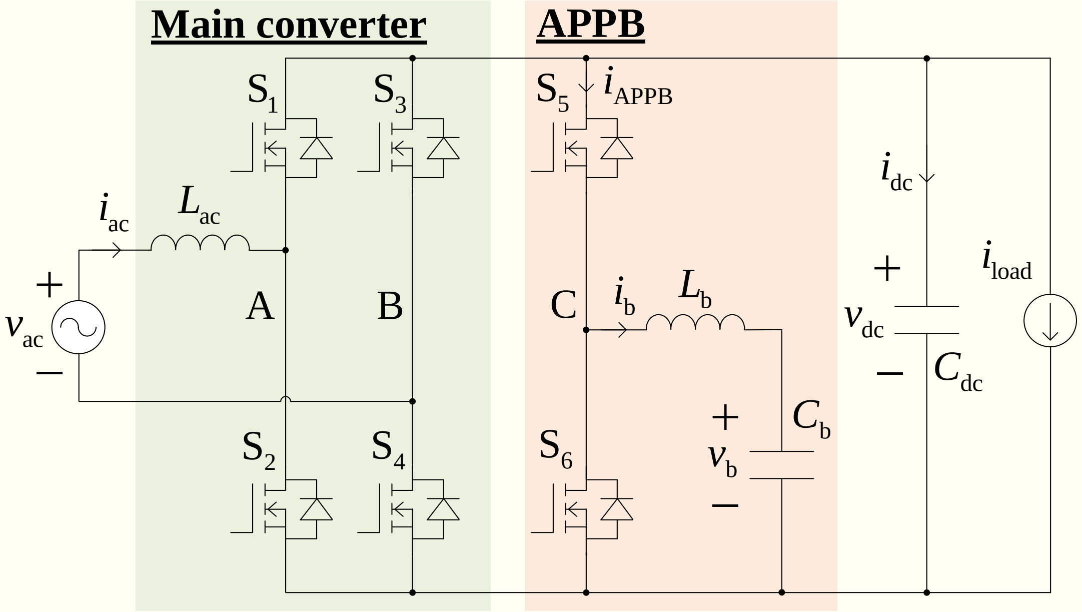

State-Space Equations

- Model:

$$\begin{cases} L_{ac}\dot{i}_{ac} = -v_{dc}m_{AB} + v_{ac} \\ C_{dc}\dot{v}_{dc} = i_{ac}m_{AB} - i_b d_C - i_{load} \\ L_b\dot{i}_b = v_{dc}d_C - v_b \\ C_b\dot{v}_b = i_b \end{cases}$$

- 4th-order system (different from the DCM case); nonlinear and coupled.

CCM: continuous conduction mode.

Instability Problem of the FLB-APD Controller

FLB-APD controller

- Select control outputs: $\mathbf{y} = [i_{\mathrm{ac}}, v_{\mathrm{dc}}]^{\mathrm{T}}$.
- Control law:

$$\begin{cases} m_{\mathrm{AB}} = \left(v_{\mathrm{ac}} - L_{\mathrm{ac}}\dot{i}_{\mathrm{ac}}^{\mathrm{R}} - \alpha_1 L_{\mathrm{ac}}(i_{\mathrm{ac}}^{\mathrm{R}} - i_{\mathrm{ac}})\right)/v_{\mathrm{dc}} \\ d_{\mathrm{C}} = \left(u_1 i_{\mathrm{ac}} - \alpha_2 C_{\mathrm{dc}}(v_{\mathrm{dc}}^{\mathrm{R}} - v_{\mathrm{dc}}) - i_{\mathrm{load}}\right)/i_{\mathrm{b}} \end{cases}$$

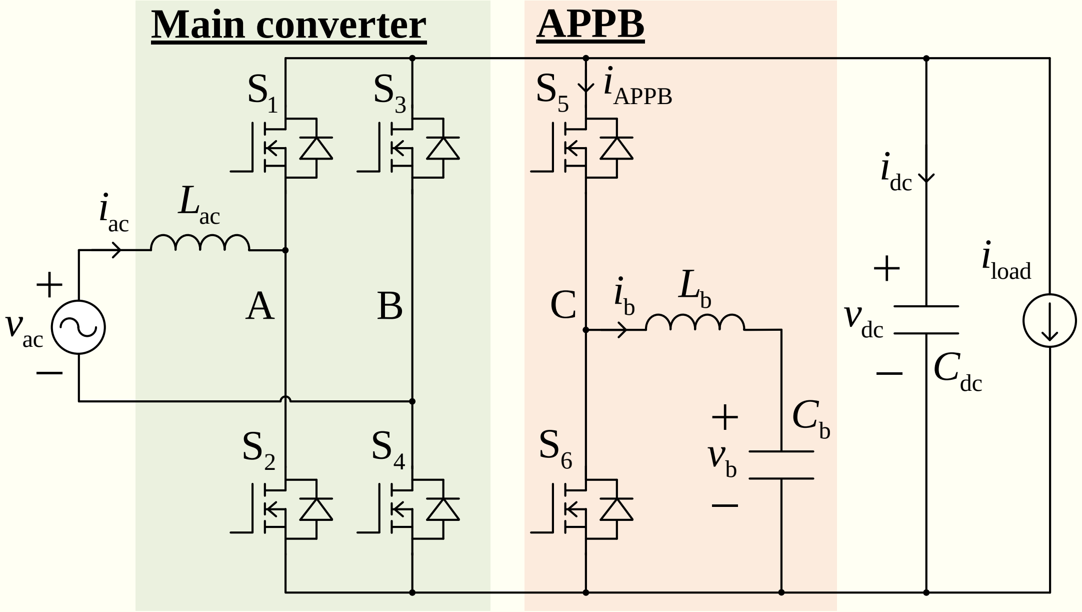

- Error dynamics of $\mathbf{y}$:

$$\dot{e}_i + \alpha_i e_i = 0 \quad \text{where} \quad e_i = y_i^{\mathrm{R}} - y_i \quad (i = 1,\ 2)$$

- Internal dynamics:

$$\begin{cases} L_{\mathrm{b}}\dot{i}_{\mathrm{b}} = p_{\mathrm{b}}/i_{\mathrm{b}} - v_{\mathrm{b}} \\ C_{\mathrm{b}}\dot{v}_{\mathrm{b}} = i_{\mathrm{b}} \end{cases} \quad \text{where} \quad p_{\mathrm{b}} = v_{\mathrm{dc}}\left(u_1 i_{\mathrm{ac}} - \alpha_2 C_{\mathrm{dc}}(v_{\mathrm{dc}}^{\mathrm{R}} - v_{\mathrm{dc}}) - i_{\mathrm{load}}\right)$$

Instability Problem of the FLB-APD Controller

FLB-APD controller

- Internal dynamics of i_b:

$$\dot{i}_b = \frac{p_b}{L_b i_b} - \frac{v_b}{L_b}$$

- Phase plane of i_b:

  - When $p_b > 0$, i_b is locally stable (the blue trace);

  - When $p_b < 0$, i_b is globally unstable (the red trace).

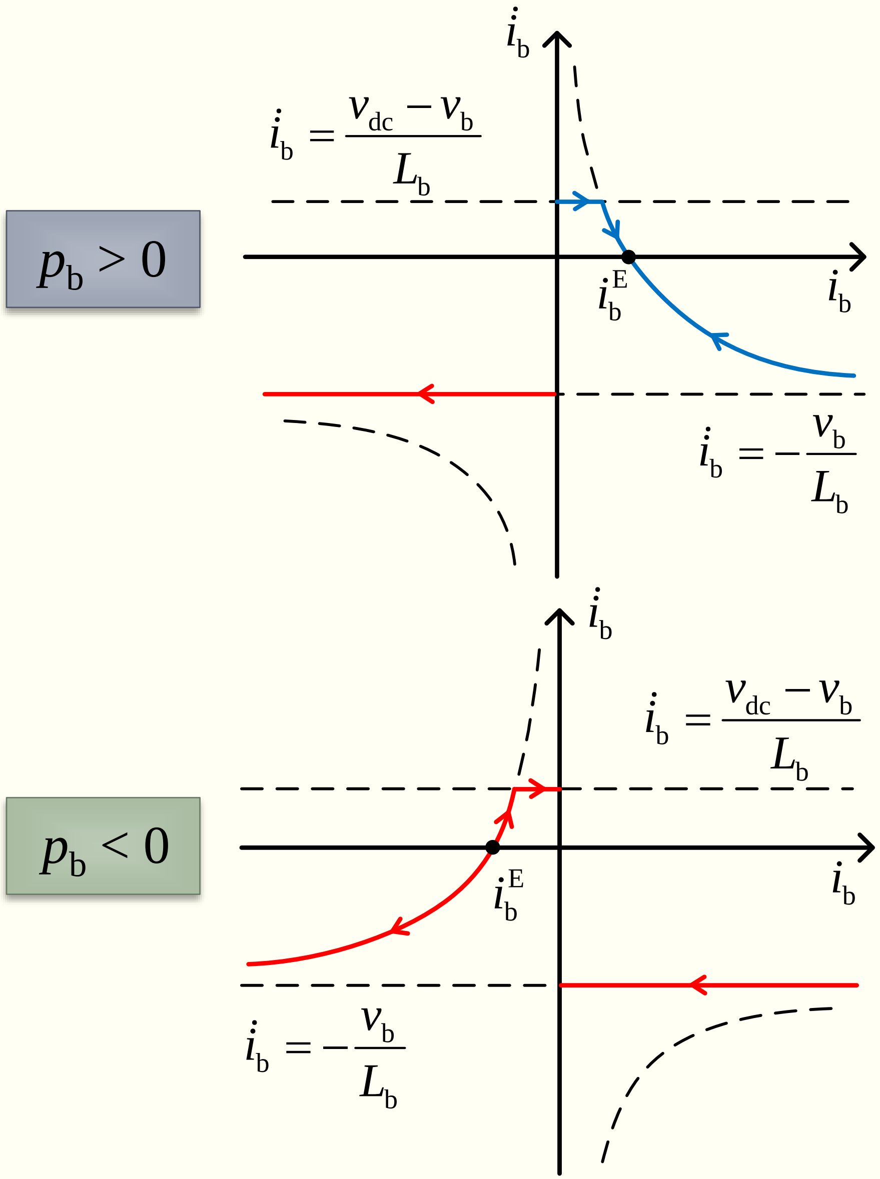

- **Summary:**

  The internal dynamics with the FLB-APD controller are unstable.

Lyapunov-Based (LB) APD Control

Modification of the FLB-APD Control Law

- Recall the system's model

$$\begin{cases} L_{\mathrm{ac}}\dot{i}_{\mathrm{ac}} = -v_{\mathrm{dc}}m_{\mathrm{AB}} + v_{\mathrm{ac}} \\ C_{\mathrm{dc}}\dot{v}_{\mathrm{dc}} = i_{\mathrm{ac}}m_{\mathrm{AB}} - i_{\mathrm{b}}d_{\mathrm{C}} - i_{\mathrm{load}} \\ L_{\mathrm{b}}\dot{i}_{\mathrm{b}} = v_{\mathrm{dc}}d_{\mathrm{C}} - v_{\mathrm{b}} \\ C_{\mathrm{b}}\dot{v}_{\mathrm{b}} = i_{\mathrm{b}} \end{cases}$$

- **Two observations**

  1) To stabilize i_{b}, d_{C} must be modified.

  2) Modification of d_{C} affects v_{dc}, whereas i_{ac} is not affected.

- **Control scheme**

  1) Use m_{AB} in the FLB-APD controller.

  2) Modify d_{C} in such a way that v_{dc} and i_{b} are simultaneously stable.

LB-APD Control

Stabilization of $\boldsymbol{v_{dc}}$ and $\boldsymbol{i_b}$ (i.e., $\boldsymbol{v_{dc} \rightarrow v_{dc}^S}$, $\boldsymbol{i_b \rightarrow i_b^S}$)

- Step 1: To use Lyapunov's method to ensure $v_{dc} \rightarrow v_{dc}^R$ (= v_{dc}^S) and $i_b \rightarrow i_b^R$;
- Step 2: To ensure $i_b^R \rightarrow i_b^S$.

Step 1 - To Ensure $v_{dc} \rightarrow v_{dc}^R$ (= v_{dc}^S) and $i_b \rightarrow i_b^R$

- Define a reference system:

$$L_b \dot{i}_b^R = v_{dc} d_C^R - v_b .$$

- Design a Lyapunov candidate function: $V(e_2, e_3) = V_1(e_2) + V_2(e_3)$

where $V_1(e_2) = \frac{1}{2} C_{dc} e_2^2 = \frac{1}{2} C_{dc} (v_{dc}^R - v_{dc})^2,\ V_2(e_3) = \frac{1}{2} L_b e_3^2 = \frac{1}{2} L_b (i_b^R - i_b)^2.$

$V \rightarrow \infty$ as $\|\mathbf{e}\| \rightarrow \infty$; $V > 0$ for all non-zero $\mathbf{e}$.

LB-APD Control

Step 1 - To Ensure $v_{dc} \rightarrow v_{dc}^{R}$ (= v_{dc}^{S}) and $i_b \rightarrow i_b^{R}$

- Make the derivative of V negative definite:

1) For $\dot{V}_2(e_3)$

By designing $d_C = \dfrac{v_b + \beta_1 e_3}{v_{dc}}$, we have $\dot{V}_2(e_3) \approx -\beta_1 e_3^2 \leq 0$.

2) For $\dot{V}_1(e_2)$

By designing $i_b^R = \dfrac{v_{dc}}{v_b}(m_{AB} i_{ac} - i_{load} - \beta_2 e_2)$, we have $\dot{V}_1(e_2) = -\beta_2 e_2^2 \leq 0$.

Thus, $\dot{V}(e_2, e_3) = \dot{V}_1(e_2) + \dot{V}_2(e_3) \leq 0$.

- $v_{dc} \rightarrow v_{dc}^{R}$ (= v_{dc}^{S}) and $i_b \rightarrow i_b^{R}$.

LB-APD Control

Step 2 - To ensure $i_b^R \to i_b^S$

- As $i_{ac} \to i_{ac}^S$, $v_{dc} \to v_{dc}^S$, and $i_b \to i_b^R$, in the steady state,

$$i_b^R \to \frac{-V_{AC}I_{AC}\cos\left(2\omega t\right) - \omega L_{ac}I_{AC}^2\sin\left(2\omega t\right)}{2\sqrt{\frac{2E_{b0}}{C_b} - \frac{V_{AC}I_{AC}}{2\omega C_b}\sin\left(2\omega t\right) + \frac{L_{ac}I_{AC}^2}{2C_b}\cos\left(2\omega t\right)}} = i_b^S$$

- Therefore, $i_b^R(t) \to i_b^S(t)$.

With Step 1 and Step 2

- v_{dc} and i_b are stabilized simultaneously.

Stability of the Remaining State v_b

- Stable According to the principle of energy conservation.

LB-APD Control

Complete Control Law

- Before modification (FLB-APD control):

$$\begin{cases} m_{AB} = (v_{ac} - v_1) / v_{dc} \\ d_C = (u_1 i_{ac} - v_2 - i_{load}) / i_b \end{cases}$$

- After modification (LB-APD control):

$$\begin{cases} m_{AB} = (v_{ac} - v_1) / v_{dc}. \quad \text{(a)} \\ d_C = \beta_1 (u_1 i_{ac} - v_2 - i_{load}) / v_b + (v_b - \beta_1 i_b) / v_{dc}. \quad \text{(b)} \end{cases}$$

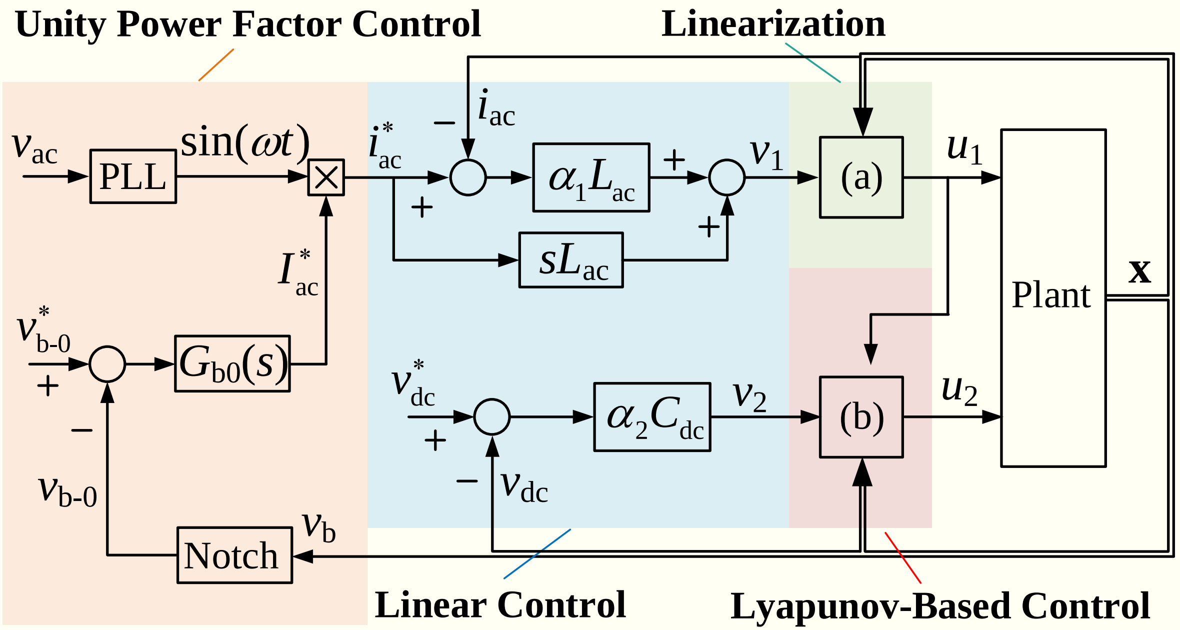

System Dynamics

- Governing equations:

$\dot{e}_i + \alpha_i e_i = 0$ where e_1, e_2, e_3 are the tracking errors of i_{ac}, v_{dc}, i_b, respectively.

- **Remark:** The desired simple dynamics of the FLB-APD control are retained.

Experimental Verification

Specifications

Parameters		Values
Rated power		300 W
Switching frequency		25 kHz
AC port	v_{ac}	220 V / 50 Hz
	L_{ac}	7 mH
DC port	v_{dc}	400 V
	C_{dc}	20 μF
APPB port	C_b	50 μF
	L_b	1.87 mH

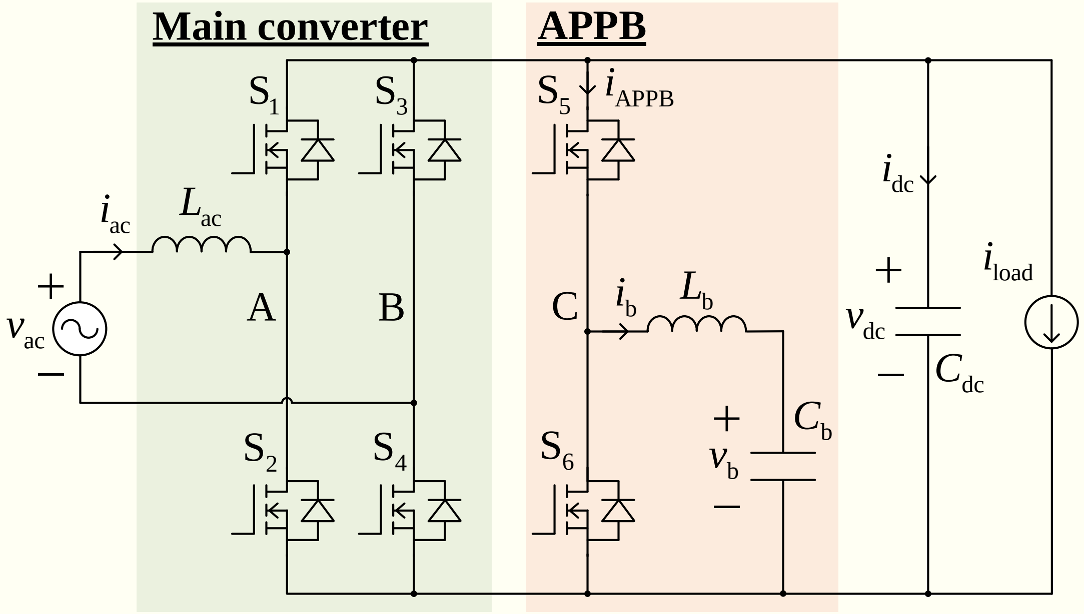

Experimental Verification

Steady-State Operation

- **AC port:**
  i) Unity power factor;
  ii) i_{ac} has a low THD of 2.21%.

- **DC port:**
  v_{dc} regulated at 400 V with a ripple of ±1%.

- **APPB port:**
  v_b has a large voltage swing of 70 V.

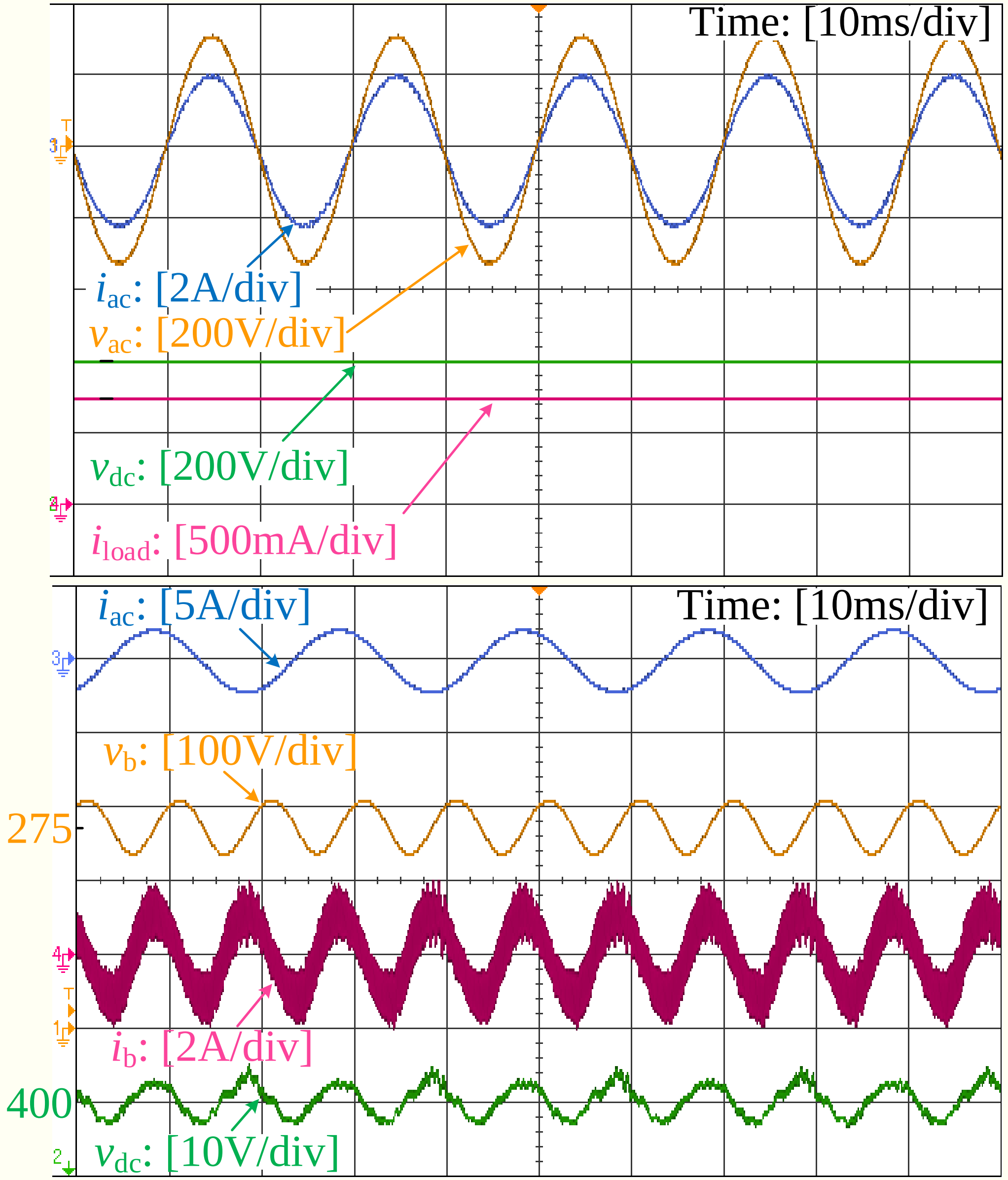

Experimental Verification

Load-Disturbance Test

- **Experiment condition:** power change - 0 W → 300 W and 300 W → 0 W.
- v_{dc} remains tightly regulated.
- i_{ac} enters its steady-state within three line cycles.
- The imbalanced power is buffered by the APPB (see v_b).

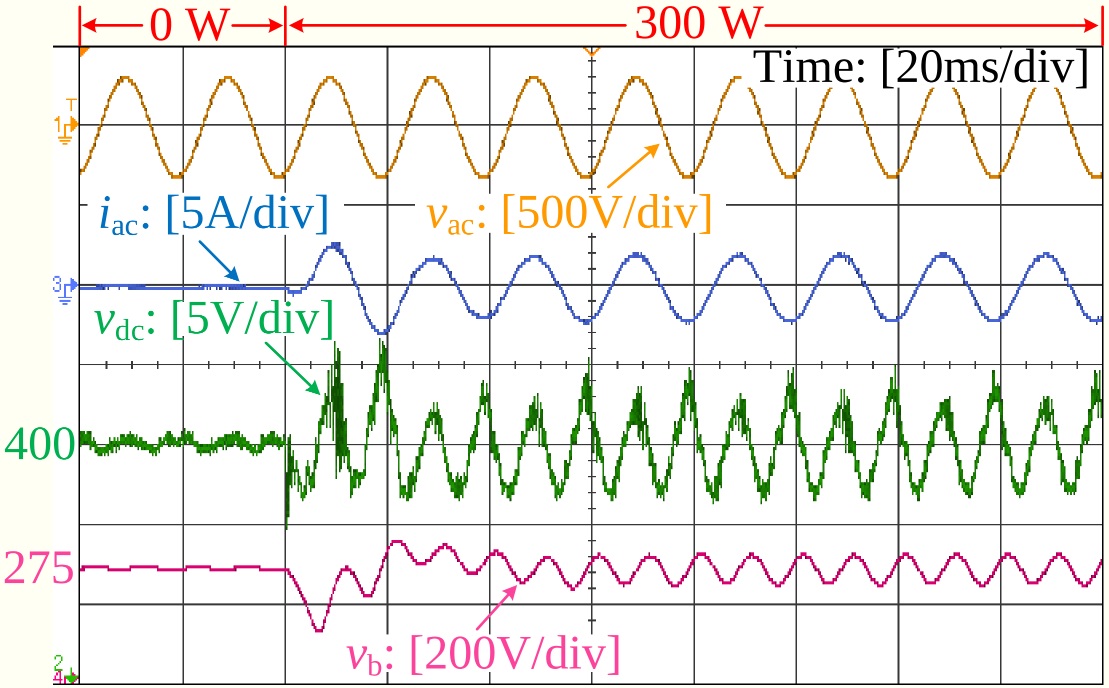

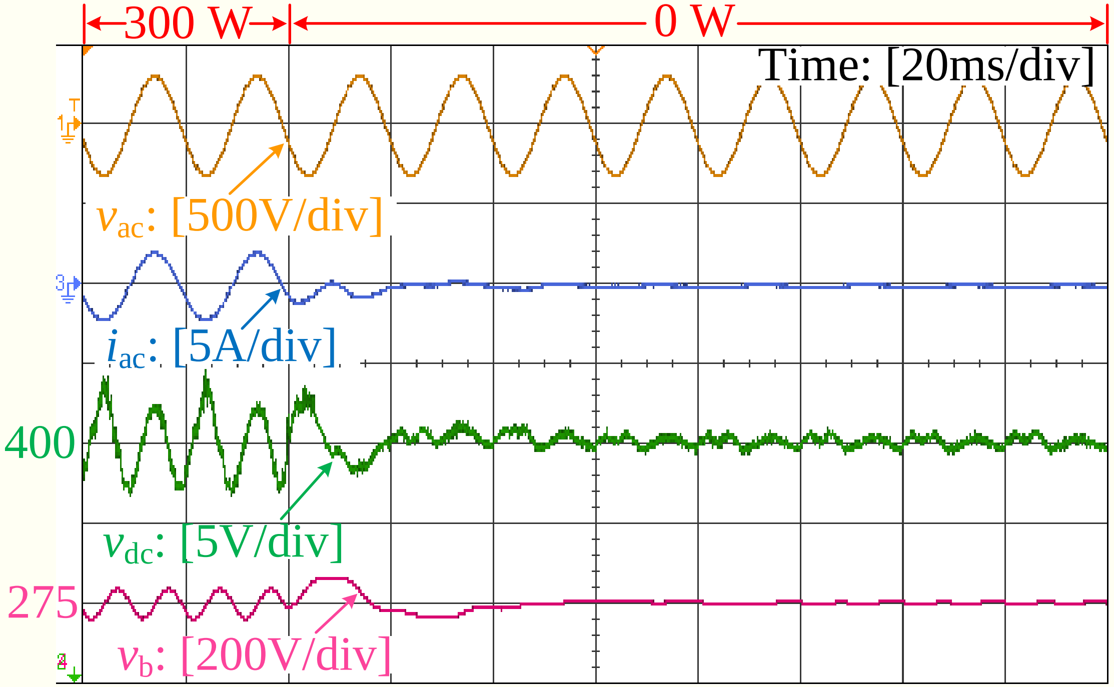

Experimental Verification

Output-Reference-Tracking Test

- **Experiment condition:**

  Reference of v_{dc}: 380 V → 420 V and 420 V → 380 V.

- v_{dc} has first-order responses with a settling time of 2 ms (designed f_{BW2} = 400 Hz).

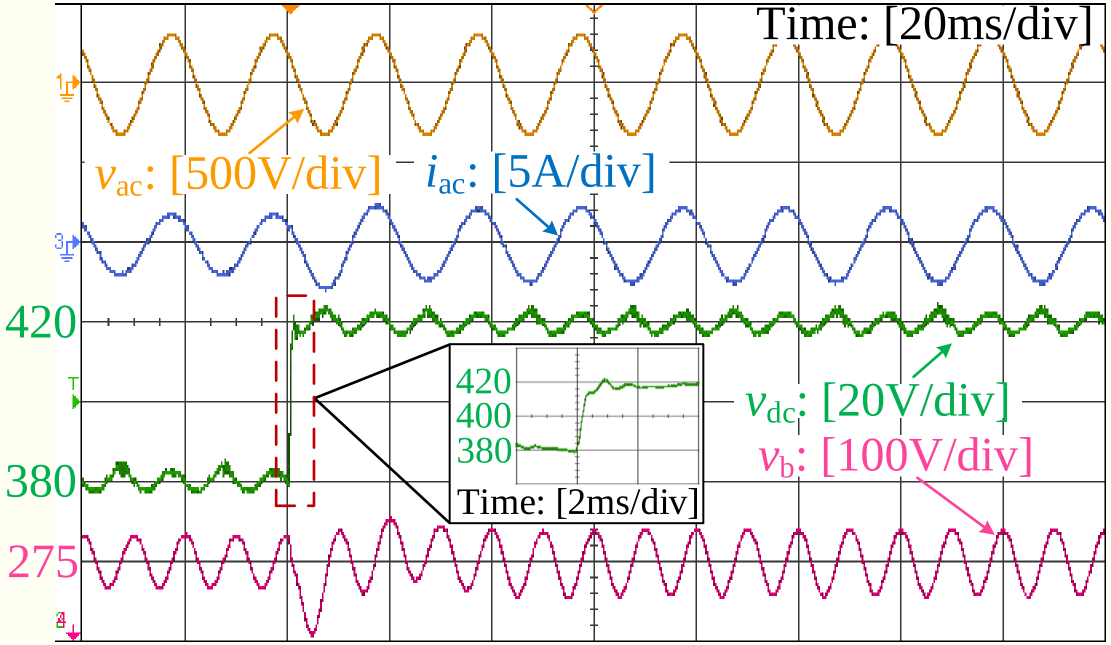

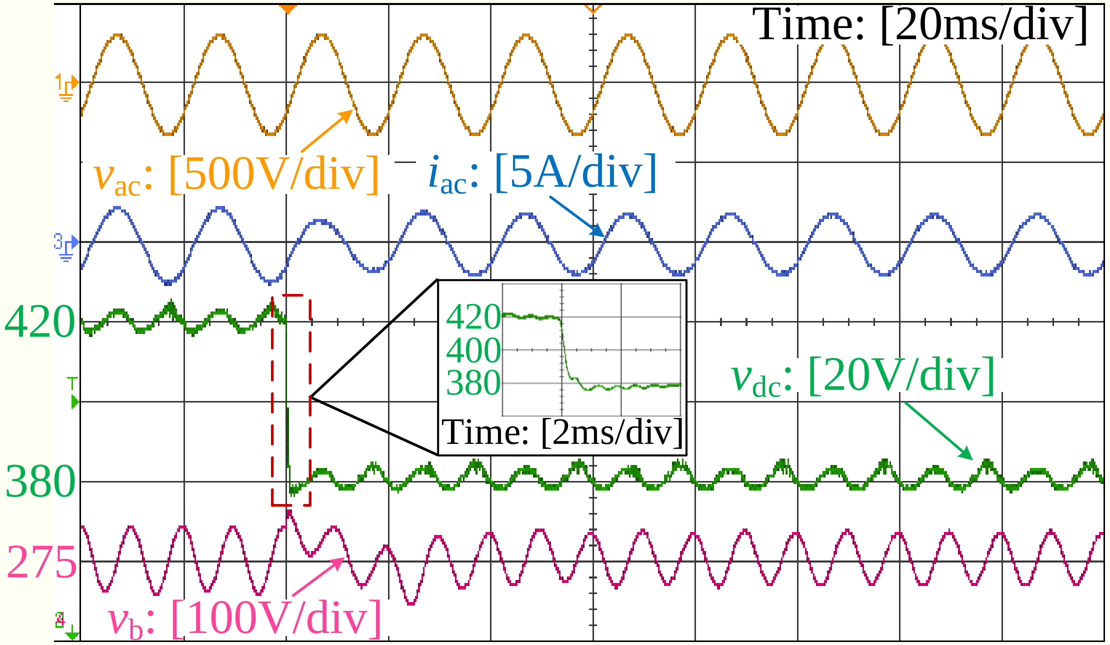

Outline

- Background of Single-Phase Converters with an APPB
- Review of Existing Control Methods
- Feedback-Linearization-Based APD Control
- Lyapunov-Based APD Control
- Sensor Count Reduction Using Algebraic Observers[19]
- Sensor Count Reduction with Simplified Algebraic Observers
- Conclusions

[19] H. Yuan, S. Li, S. -C. Tan, and S. Y. R. Hui, “Sensor count reduction for single-phase converters with an active power buffer using algebraic observers,” *IEEE Trans. Ind. Electron.*, vol. 68, no. 11, pp. 10666–10676, Nov. 2021.

High Sensor Count Problem

Example Circuit

- Topology: full-bridge rectifier + buck-type APPB.
- The APPB operates in the CCM.

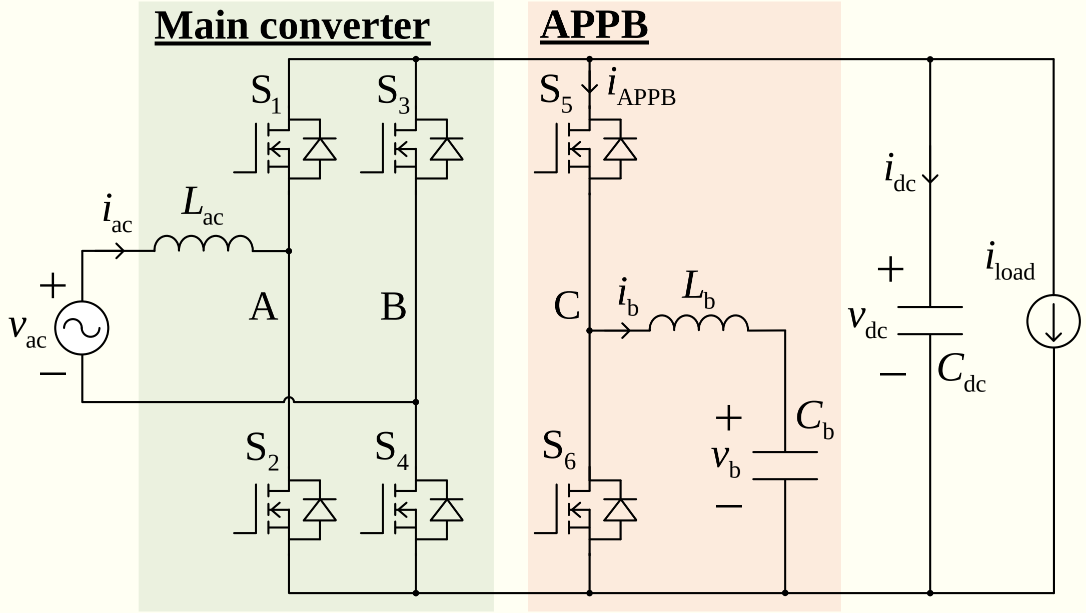

Mathematical Modeling

- State-space equations:

$$\begin{cases} \mathbf{C}\dot{\mathbf{x}} = \mathbf{J}(\mathbf{x},\mathbf{u},\mathbf{v}) \\ \mathbf{y} = \mathbf{K}\mathbf{x} \end{cases}$$

where

$$\mathbf{C} = \begin{bmatrix} L_{ac} & 0 & 0 & 0 \\ 0 & C_{dc} & 0 & 0 \\ 0 & 0 & L_b & 0 \\ 0 & 0 & 0 & C_b \end{bmatrix}, \mathbf{K} = \begin{bmatrix} 1 & 0 & 0 & 0 \\ 0 & 1 & 0 & 0 \\ 0 & 0 & 1 & 0 \end{bmatrix}, \mathbf{J}(\mathbf{x},\mathbf{u},\mathbf{v}) = \begin{bmatrix} v_{ac} - m_{AB} v_{dc} \\ m_{AB} i_{ac} - d_C i_b - i_{load} \\ d_C v_{dc} - v_b \\ i_b \end{bmatrix}.$$

High Sensor Count Problem

Sensor Requirement

- For an n^{th}-order system with m external disturbance sources, $n+m$ sensors are generally required for full state feedback control.
- Example converter (4^{th}-order) vs. conventional converter without the APPB (2^{nd}-order)

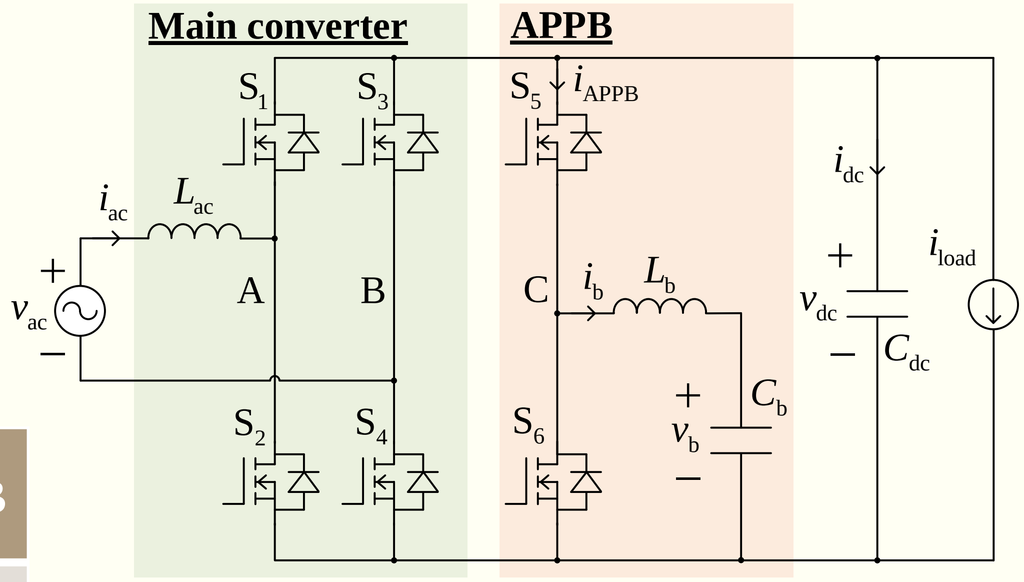

To measure	Purpose of sensing	With APPB	Without APPB
i_{ac}	Grid current control	√	√
i_{load}	Load disturbance rejection	suggested (√)	unnecessary (×)
i_b	APPB power control	√	×
v_{ac}	Grid phase information	√	√
v_{dc}	DC-link voltage regulation	√	√
v_b	APPB energy control	√	×
		6 sensors	3 sensors

The sensor count is high in the single-phase converter with an APPB.

High Sensor Count Problem

Problems of High Sensor Count

- Compromise the system volume and cost.
- Undermine the system reliability.

Algebraic Estimation – A New Method[20]

- Fast dynamics and no convergence issues[21].
- A wide application range, including a wide class of nonlinear systems[22].

Objective of This Part

- To introduce the theory of employing algebraic observers to reduce the number of sensors.

[20] M. Fliess, and H. Sira–Ramírez, "An algebraic framework for linear identification," in *Proc. ESAIM, Control, Optim. Calc. Var.*, 2003, pp. 151–168.
[21] A. Gensior, J. Weber, J. Rudolph, and H. Guldner, "Algebraic parameter identification and asymptotic estimation of the load of a boost converter," *IEEE Trans. Ind. Electron.*, 55(9), pp. 3352–3360, Sept. 2008
[22] H. Sira-Ramirez, C. Garcia-Rodriguez, J. Cortes-Romero, and A. Luviano-Juarez, *Algebraic identification and estimation methods in feedback control systems*, 1st ed., The Atrium Southern Gate, SXW, UK: John Wiley & Sons Ltd, pp. 71–144, 2014.

Sensor Count Reduction Using Algebraic Observers

Principle of Algebraic Observers

- System's model:

$$\begin{cases} \mathbf{C}\dot{\mathbf{x}} = \mathbf{J}(\mathbf{x},\mathbf{u},\mathbf{v}) \\ \mathbf{y} = \mathbf{K}\mathbf{x} \end{cases} \qquad (1)$$

(**u** and **y** are known.)

- Decompose the right-hand side of input-output model:

$$\dot{\mathbf{y}} = \mathbf{K}\mathbf{C}^{-1}\mathbf{J}(\mathbf{x},\mathbf{u},\mathbf{v}) = \boldsymbol{\lambda}(\mathbf{x},\mathbf{u},\mathbf{v}) + \mathbf{f}(\mathbf{y},\mathbf{u}) \qquad (2)$$

(**f** are known, while $\boldsymbol{\lambda}$ are to be estimated.)

- $\boldsymbol{\lambda}$ can be readily estimated from (2) as:

$$\boldsymbol{\lambda}(\mathbf{x},\mathbf{u},\mathbf{v}) = \dot{\mathbf{y}} - \mathbf{f}(\mathbf{y},\mathbf{u}) \qquad (3)$$

- **Remarks on (3):**

1) Open-loop estimation;
2) The selection of $\boldsymbol{\lambda}$ is flexible;
3) Using (3) is subject to noise problems.

Sensor Count Reduction Using Algebraic Observers

Smoothing the Noises

- Use a piecewise constant term $\hat{\boldsymbol{\lambda}}$ to approximate $\boldsymbol{\lambda}$. By applying Laplace transform to (3), we have

$$\frac{\hat{\boldsymbol{\lambda}}}{s} = s\mathbf{Y}(s) - \mathbf{y}(0) - \mathbf{F}(s) \qquad (4)$$

- With manipulation of the i^{th} row of (4), we have

$$(-1)^{n_i} \cdot n_i ! \cdot \frac{\hat{\lambda}_i}{s^{m_i+n_i+1}} = \frac{n_i}{s^{m_i}} \frac{d^{n_i-1}Y_i(s)}{ds^{n_i-1}} + \frac{1}{s^{m_i-1}} \frac{d^{n_i}Y_i(s)}{ds^{n_i}} - \frac{1}{s^{m_i}} \frac{d^{n_i}F_i(s)}{ds^{n_i}}. \qquad (5)$$

- In the time domain, we have:

$$\hat{\lambda}_i(t) = \begin{cases} \dfrac{n_i+1}{T_i^{n_i+1}} \left[T_i^{n_i} y_i(t) - \int_{t-T_i}^{t} (\sigma + T_i - t)^{n_i-1} \left(n_i y_i(\sigma) + (\sigma + T_i - t) f_i(\sigma) \right) d\sigma \right], & m_i = 1 \\ \dfrac{(m_i+n_i)!}{n_i ! \cdot (m_i-2)! \cdot T_i^{m_i+n_i}} \int_{t-T_i}^{t} (t-\sigma)^{m_i-2} (\sigma + T_i - t)^{n_i-1} \left[\left(\sigma + T_i - t - \dfrac{n_i(t-\sigma)}{m_i-1} \right) y_i(\sigma) - \dfrac{(\sigma+T_i-t)(t-\sigma)}{m_i-1} f_i(\sigma) \right] d\sigma, & m_i \geq 2 \end{cases} \qquad (6)$$

No derivative terms, hence improved signal-to-noise ratio (SNR).

Sensor Count Reduction Using Algebraic Observers

Estimation Accuracy of the Algebraic Observers

- The error due to the piecewise constant approximation is analyzed.

- The Laplace transform of (3) without making the piecewise constant approximation is

$$\mathbf{\Lambda}(s) = s\mathbf{Y}(s) - \mathbf{y}(0) - \mathbf{F}(s) \qquad (7)$$

- By comparing the equations with and w/o the approximation, we can relate $\hat{\boldsymbol{\lambda}}$ to $\mathbf{\Lambda}(s)$ as

$$\frac{1}{s^{m_i}} \frac{d^{n_i}\Lambda_i(s)}{ds^{n_i}} = (-1)^{n_i} \cdot n_i! \cdot \frac{\hat{\lambda}_i}{s^{m_i+n_i+1}} \qquad (8)$$

- In the time domain,

$$\hat{\lambda}_i(t) = \frac{(m_i+n_i)!}{(m_i-1)! \cdot n_i! \cdot T_i^{m_i+n_i}} \int_{t-T_i}^{t} (t-\sigma)^{m_i-1}(T_i - t + \sigma)^{n_i} \lambda_i(\sigma) d\sigma \qquad (9)$$

- The transfer function of the observer: $H_i(s) = \dfrac{\hat{\Lambda}_i(s)}{\Lambda_i(s)} = \kappa_i e^{-\tau_i s}$.

Sensor Count Reduction Using Algebraic Observers

Estimation Accuracy of the Algebraic Observers

- Simplified results when T_i is small:

$$\kappa_i \approx 1,\ \ \tau_i \approx \frac{m_i}{m_i + n_i + 1} T_i. \qquad (10)$$

Remarks:

1) $\hat{\lambda}_i$ has almost identical magnitude to that of λ_i.

2) The larger the m_i, the longer the time delay;

3) The larger the n_i, the shorter the time delay;

4) Time delay is proportional to T_i;

5) $\tau_i < T_i$;

Transfer function:

$$H_i(s) = \frac{\hat{\Lambda}_i(s)}{\Lambda_i(s)} = \kappa_i e^{-\tau_i s}$$

- The algebraic observer can be optimized by properly designing m_i, n_i, and T_i.

Illustration of Algebraic Observer Design

LB-APD Control as an Example

- Control law:

$$\begin{cases} m_{AB} = \dfrac{1}{v_{dc}}\left(v_{ac} - L_{ac}\dot{i}_{ac}^{R} - \beta_1\left(i_{ac}^{R} - i_{ac}\right)\right) \\ d_C = \dfrac{\beta_3}{v_b}\left(m_{AB}i_{ac} - i_{load} - \beta_2\left(v_{dc}^{R} - v_{dc}\right)\right) + \dfrac{1}{v_{dc}}\left(v_b - \beta_3 i_b\right) \end{cases}$$

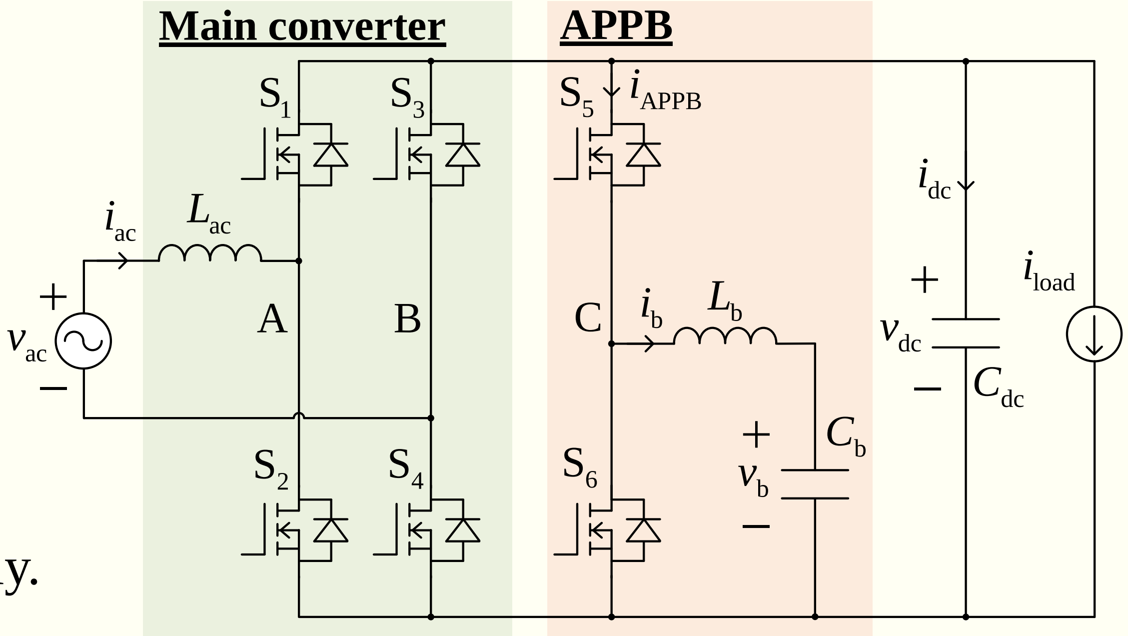

- System dynamics (decoupled and first-order):

$$\dot{e}_j + \alpha_j e_j = 0$$

e_1, e_2, e_3 are the tracking errors of i_{ac}, v_{dc}, i_b, respectively.

- Require 6 sensors: v_{ac}, v_{dc}, v_b, i_{ac}, i_b, i_{load}.

Illustration of Algebraic Observer Design

Procedure of Designing Algebraic Observers

1) Obtain **u** from the control law and **y** from sensors.

2) Select $\boldsymbol{\lambda}$ and **f**: $\boldsymbol{\lambda} = \{\bar{\mathbf{x}}_\mathbf{y}, \mathbf{v}\}$, $\mathbf{f} = \mathbf{K}\mathbf{C}^{-1}\mathbf{J} - \boldsymbol{\lambda}$, e.g.,

$$\boldsymbol{\lambda} = \begin{bmatrix} v_{\mathrm{ac}} \\ m_{\mathrm{AB}} i_{\mathrm{ac}} - i_{\mathrm{load}} \\ v_{\mathrm{b}} \end{bmatrix}, \ \mathbf{f} = \begin{bmatrix} -m_{\mathrm{AB}} v_{\mathrm{dc}} \\ -d_{\mathrm{C}} i_{\mathrm{b}} \\ -d_{\mathrm{C}} v_{\mathrm{dc}} \end{bmatrix}.$$

3) Estimate $\boldsymbol{\lambda}$ using the algebraic observers.

4) Finalize the control law

$$\begin{cases} m_{\mathrm{AB}} = \dfrac{1}{v_{\mathrm{dc}}}\left(\hat{\lambda}_1 - L_{\mathrm{ac}} \dot{i}_{\mathrm{ac}}^{\mathrm{R}} - \beta_1\left(i_{\mathrm{ac}}^{\mathrm{R}} - i_{\mathrm{ac}}\right)\right) \\ d_{\mathrm{C}} = \dfrac{\beta_3}{\hat{\lambda}_3}\left(\hat{\lambda}_2 - \beta_2\left(v_{\mathrm{dc}}^{\mathrm{R}} - v_{\mathrm{dc}}\right)\right) + \dfrac{1}{v_{\mathrm{dc}}}\left(\hat{\lambda}_3 - \beta_3 i_{\mathrm{b}}\right) \end{cases}$$

Require 3 sensors: v_{dc}, i_{ac}, i_{b}.

Overall control block diagram

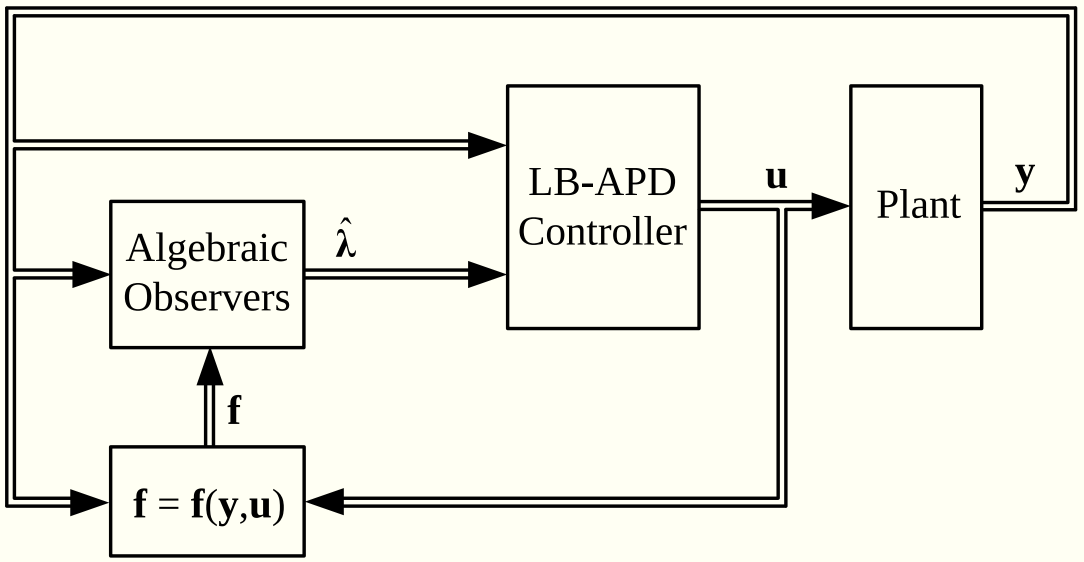

Experimental Verification

System Specifications

Parameters		Values
Rated power		300 W
Switching frequency		25 kHz
AC port	v_{ac}	220 V / 50 Hz
	L_{ac}	7 mH
DC port	v_{dc}	400 V
	C_{dc}	20 μF
PPB port	C_b	50 μF
	L_b	1.87 mH

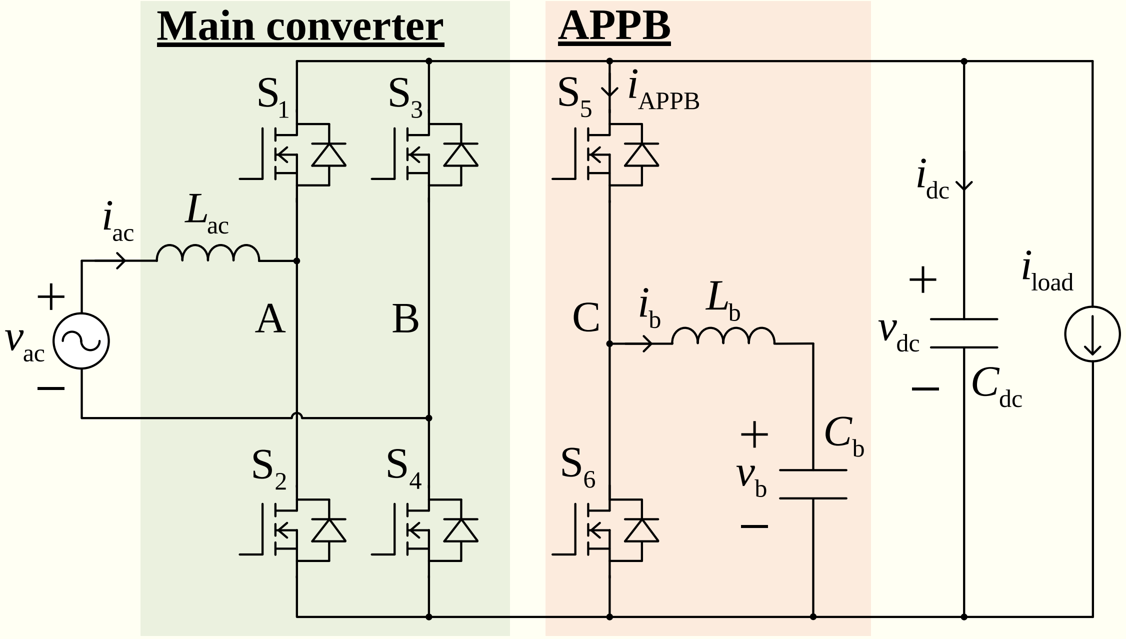

Experimental Verification

Performance of the Algebraic Observers

- **λ** are estimated with relatively small errors.

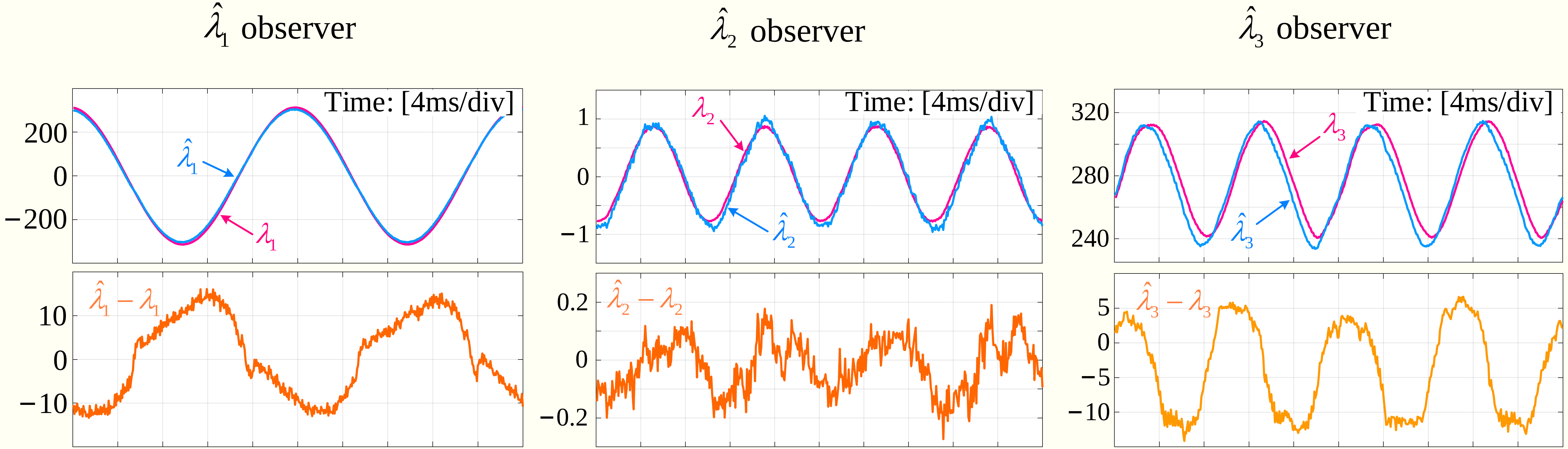

Experimental Verification

Performance of the Closed-Loop System

- **Experiment condition:** Steady-state operation (300 W).

- **AC port:**

  1) Unity power factor;

  2) i_{ac} has a low THD of 2.60%.

- **DC port:**

  v_{dc} regulated at 400 V with a ripple of ±1%.

- **APPB port:**

  v_b has a large voltage swing of 70 V.

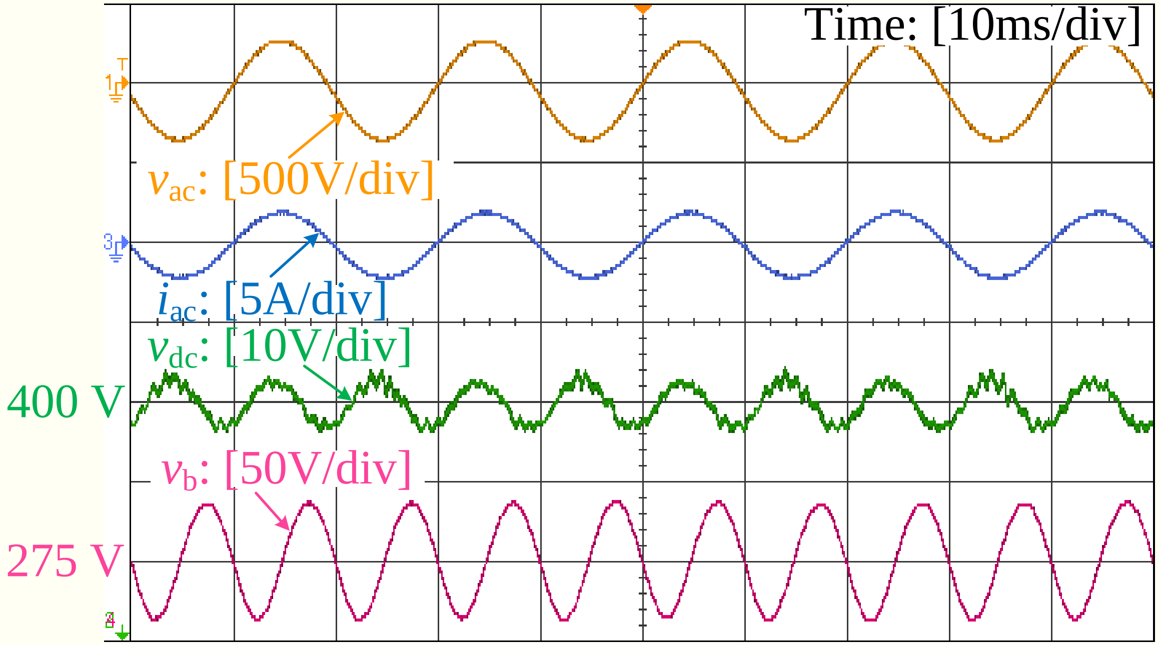

Experimental Verification

Performance of the Closed-Loop System

- **Experiment condition:** Load power change: 0 W → 300 W and 300 W → 0 W.
- v_{dc} remains tightly regulated in the range of (400 ± 5) V.
- i_{ac} enters its steady-state within three line cycles.
- The algebraic-observer-based controller is robust against load disturbances.

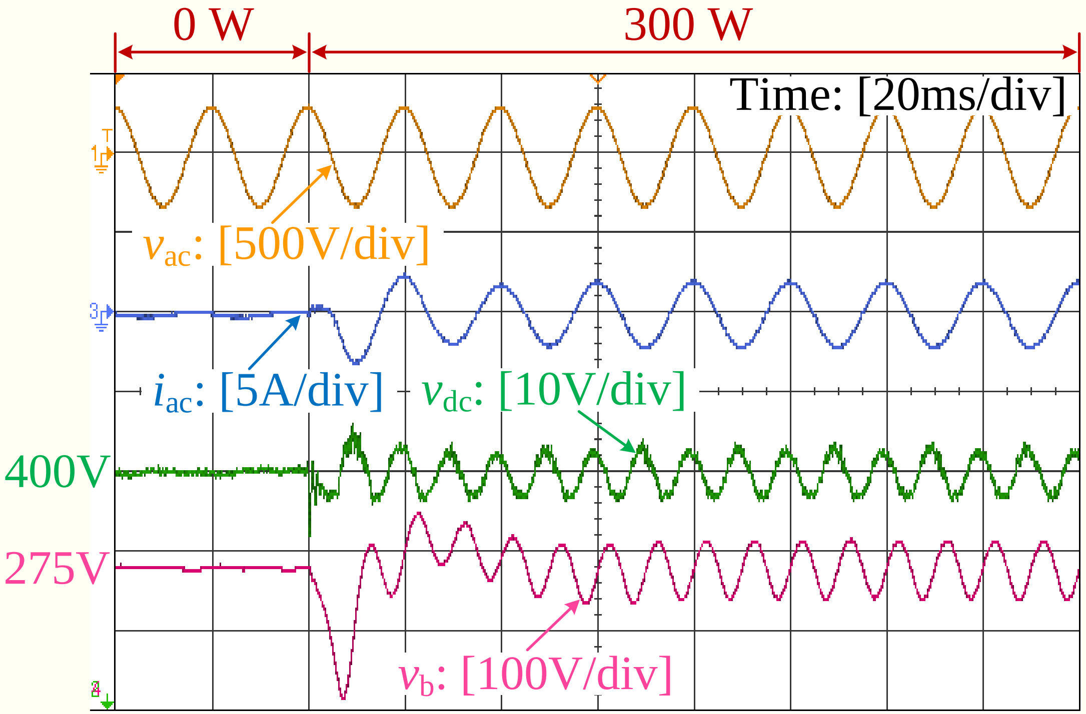

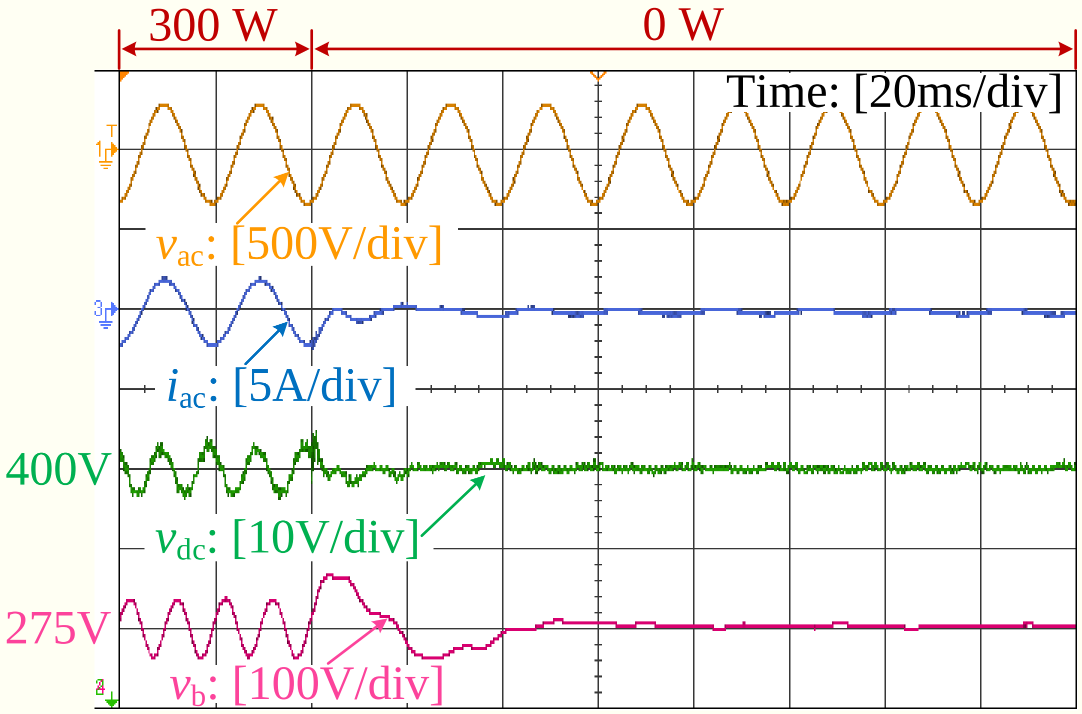

Experimental Verification

Performance of the Closed-Loop System

- **Experiment condition -** Reference of v_{dc}: 380 V → 420 V and 420 V → 380 V.
- v_{dc} has first-order responses with a settling time of 3 ms (designed f_{BW2} = 300 Hz).
- The simple dynamics of the original controller are retained.

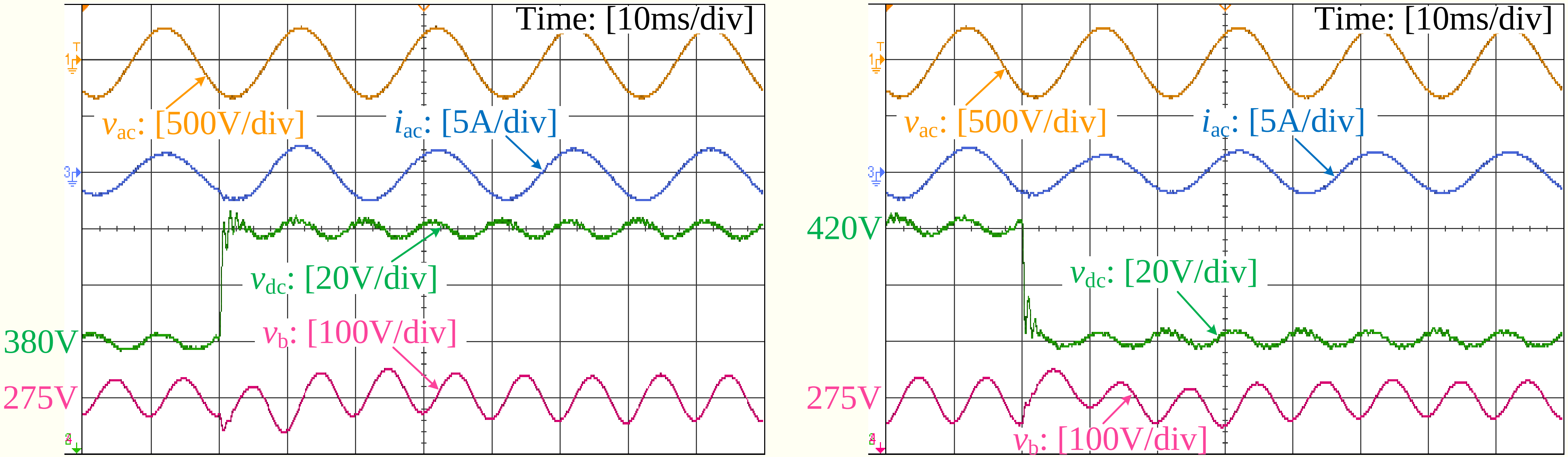

Outline

- Background of Single-Phase Converters with an APPB
- Review of Existing Control Methods
- Feedback-Linearization-Based APD Control
- Lyapunov-Based APD Control
- Sensor Count Reduction Using Algebraic Observers
- Sensor Count Reduction with Simplified Algebraic Observers[23]
- Conclusions

[23] H. Yuan, S. Li, S. -C. Tan, and R. S. -Y. Hui, “Simplified algebraic estimation technique for sensor count reduction in single-phase converters with an active power buffer,” *IEEE Trans Power Electron.*, vol. 36, no. 10, pp. 11444–11455, Oct. 2021.

Introduction

Limitations of Algebraic-Observer-Based Sensor Reduction Method

- The design of algebraic observers is not straightforward.
- Real-time computation is non-trivial.

Objectives of This Part

- To present a simplified algebraic observer that has the following advantages:
  1) applicable to different topologies;
  2) intuitive design;
  3) extremely low computational complexity.
- To employ the simplified algebraic observers to reduce the number of sensors in single-phase converters with an APPB.

Simplified Algebraic Observers

Computational Burden of Original Algebraic Observer

- Discretized algebraic observer:

$$\hat{\lambda}_{i,z}[k] = \sum_{p=0}^{q_i} k_{xi}(p) y_{i,z}[k-q_i+p] + \sum_{p=1}^{q_i} k_{fi}(p) f_{i,z}[k-q_i+p]$$

- **Remarks:**

1) $(2q_i + 1)$ multiplications and $2q_i$ additions are required;

2) The design of $q_i > 10$ is typical[24]–[26];

3) q_i should be minimized to reduce the computational burden.

4) When $q_i = 1$, the computational burden is most simplified. The observer reduces to $\boldsymbol{\lambda}(\mathbf{x},\mathbf{u},\mathbf{v}) = \dot{\mathbf{y}} - \mathbf{f}(\mathbf{y},\mathbf{u})$ which, however, is noise-sensitive.

[24] A. Gensior, J. Weber, J. Rudolph, and H. Guldner, “Algebraic parameter identification and asymptotic estimation of the load of a boost converter,” *IEEE Trans. Ind. Electron.*, 55(9), pp. 3352–3360, Sept. 2008

[25] H. Sira-Ramirez, C. Garcia-Rodriguez, J. Cortes-Romero, and A. Luviano-Juarez, *Algebraic identification and estimation methods in feedback control systems*, 1st ed., The Atrium Southern Gate, SXW, UK: John Wiley & Sons Ltd, pp. 71–144, 2014.

[26] H. Li, H. Zhang, Y. Zhou, and S. Zeng, "Cascaded proportional control with algebraic estimators for PFC AC/DC converters," *IEEE Trans. Power Electron.*, vol. 34, no. 12, pp. 12504–12512, Dec. 2019.

Simplified Algebraic Observers

Principle of Simplified Algebraic Observer

- Employ an LPF* to smooth the noise:

$$\hat{\boldsymbol{\lambda}}' = \left(\left(\dot{\mathbf{y}} - \mathbf{f}(\mathbf{y}, \mathbf{u})\right) * h_{\mathrm{LPF}}\right)$$

- **Design of LPF:**
  1) The cutoff frequency f_c should satisfy $f_{est} << f_c << f_s$ for accurate estimation and sufficient noise suppression;
  2) $f_c >> f_{BW}$ for minimizing the influence of the observer on the controller.

The design of the observer is largely simplified.

Original Algebraic Observer

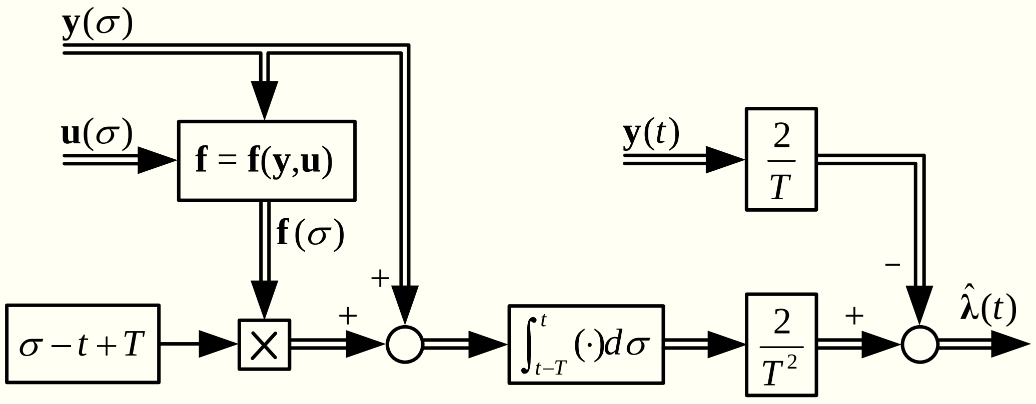

Simplified Algebraic Observer

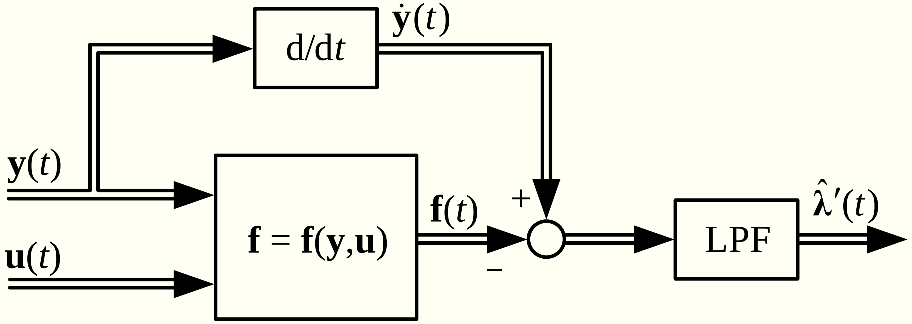

LPF: low pass filter.

Comparison of the Original and Simplified Observers

Performance

- Transfer function of the original observer:

$$H_{\mathrm{AO1}}(s) = \kappa(\omega)e^{-\tau(\omega)s}$$

where

$$\kappa(\omega)=2\sqrt{(1-\cos(\omega T))^2+(\omega T-\sin(\omega T))^2}/(\omega^2 T^2)$$

$$\tau(\omega) = \arctan((\omega T-\sin(\omega T))/(1-\cos(\omega T)))/\omega$$

- Transfer function of the simplified observer

$$H_{\mathrm{AO2}}(s) = 2\pi f_{\mathrm{c}}/(s+2\pi f_{\mathrm{c}})$$

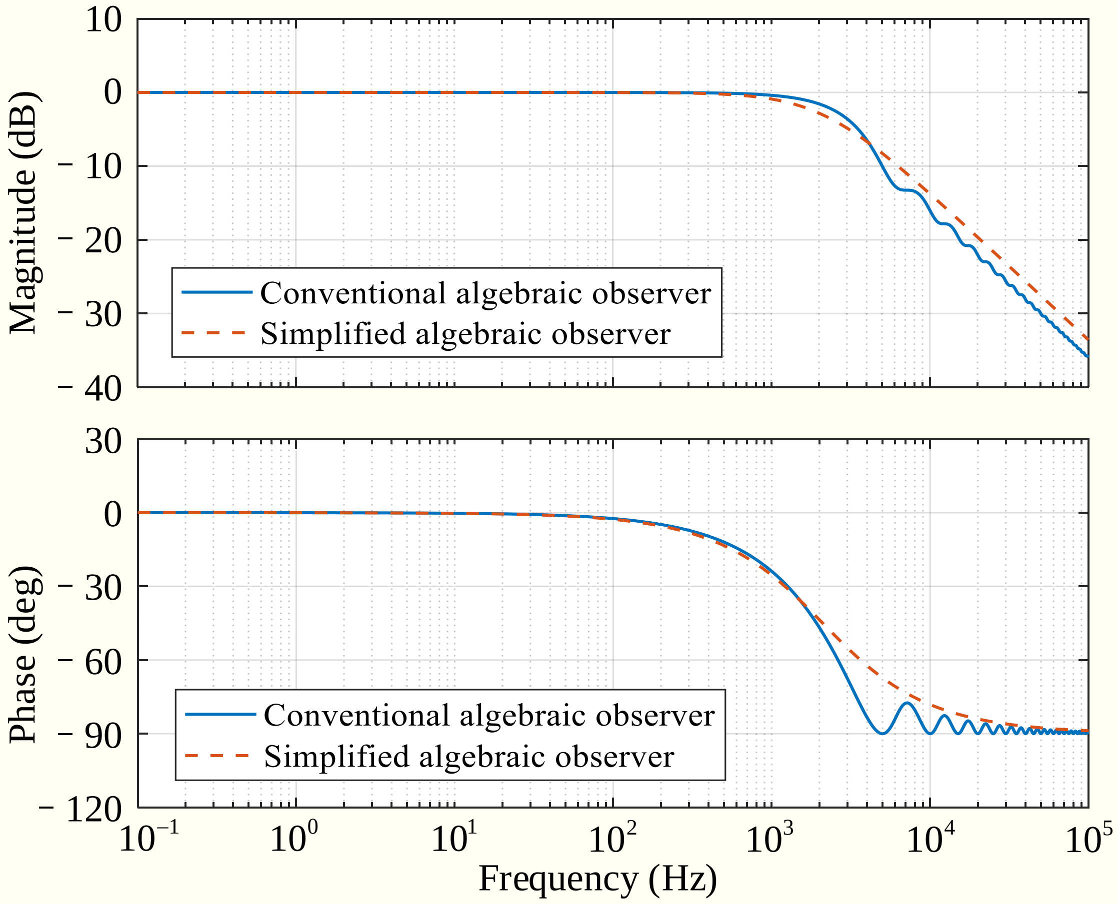

- Results:
  1) Similar estimation performances for low-frequency signals;
  2) Estimation accuracy drops for medium-frequency signals;
  3) Similar noise-suppression capabilities.

Comparison of the Original and Simplified Observers

Computational Complexity

- Original observer:

  $2q_i$ multiplication and $2q_i$+1 addition operators.

- Simplified observer:

$$\hat{\boldsymbol{\lambda}}'_{\mathrm{d}}[k] = m_1 \hat{\boldsymbol{\lambda}}'_{\mathrm{d}}[k-1] + m_2 \left(\mathbf{w}_{\mathrm{d}}[k] + \mathbf{w}_{\mathrm{d}}[k-1]\right), \quad \mathbf{w}_{\mathrm{d}}[k] = \frac{1}{T_{\mathrm{s}}}\left(\mathbf{y}_{\mathrm{d}}[k] - \mathbf{y}_{\mathrm{d}}[k-1]\right) - \mathbf{f}_{\mathrm{d}}[k]$$

  with $m_1 = \dfrac{1-\pi f_{\mathrm{c}} T_{\mathrm{s}}}{1+\pi f_{\mathrm{c}} T_{\mathrm{s}}}, \quad m_2 = \dfrac{\pi f_{\mathrm{c}} T_{\mathrm{s}}}{1+\pi f_{\mathrm{c}} T_{\mathrm{s}}}$

  3 multiplication and 4 addition operators.

- The simplified observer outperforms the original one with respect to:
  1) computational efficiency when $q_i > 1$.
  2) design simplicity due to decoupled noise-suppression performance and computational burden.

Experimental Verification

System Specifications

Parameters		Values
Rated power		300 W
Switching frequency		25 kHz
AC port	v_{ac}	220 V / 50 Hz
	L_{ac}	7 mH
DC port	v_{dc}	400 V
	C_{dc}	25 μF
PPB port	C_b	50 μF
	L_b	1.87 mH

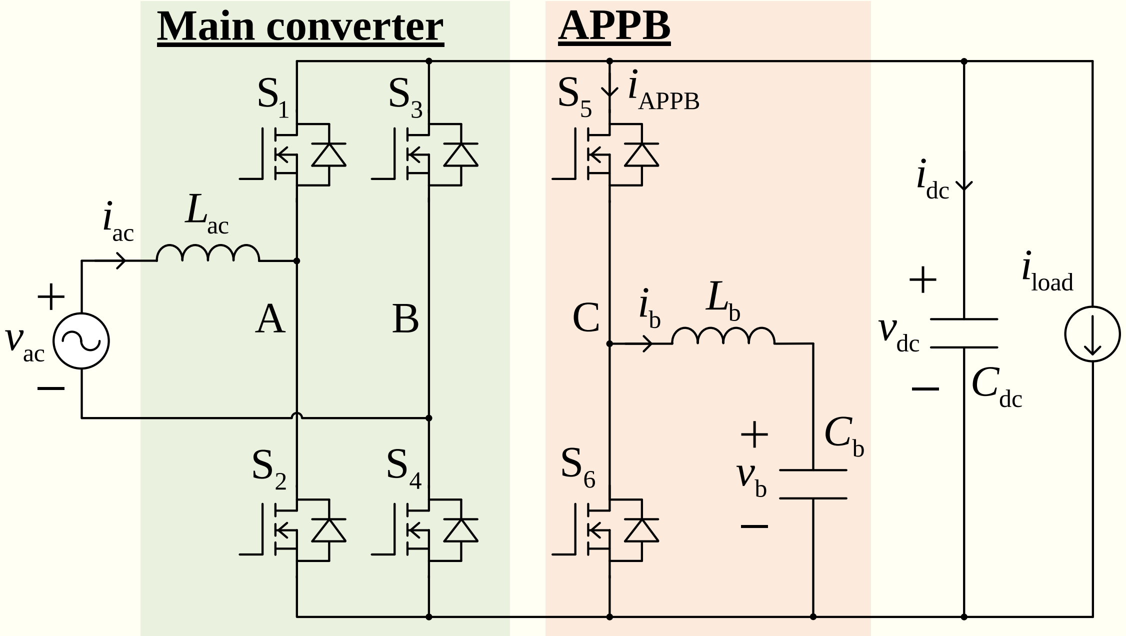

Experimental Verification

Comparison of the Performances

- λ are estimated with relatively small errors.
- The original observers and the simplified observers achieve similar estimation performances.

$\hat{\lambda}_1$ and $\hat{\lambda}_1'$ observers

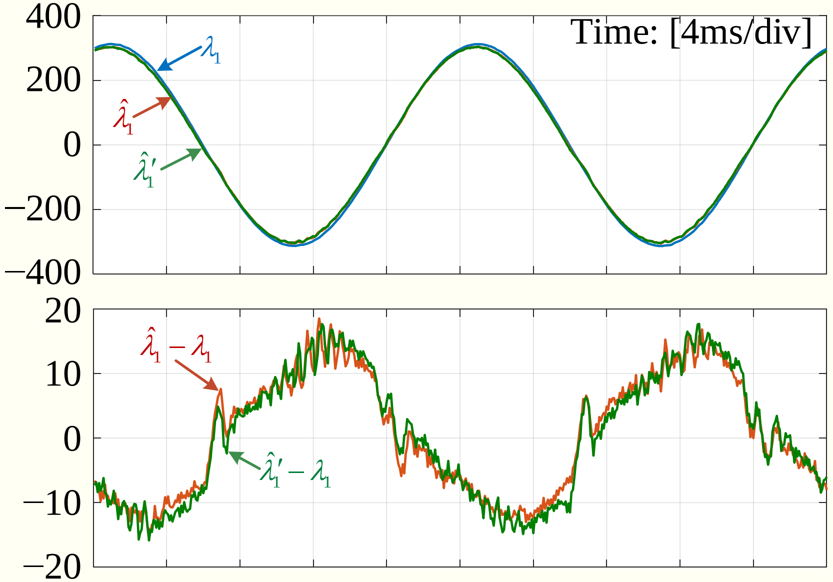

$\hat{\lambda}_2$ and $\hat{\lambda}_2'$ observers

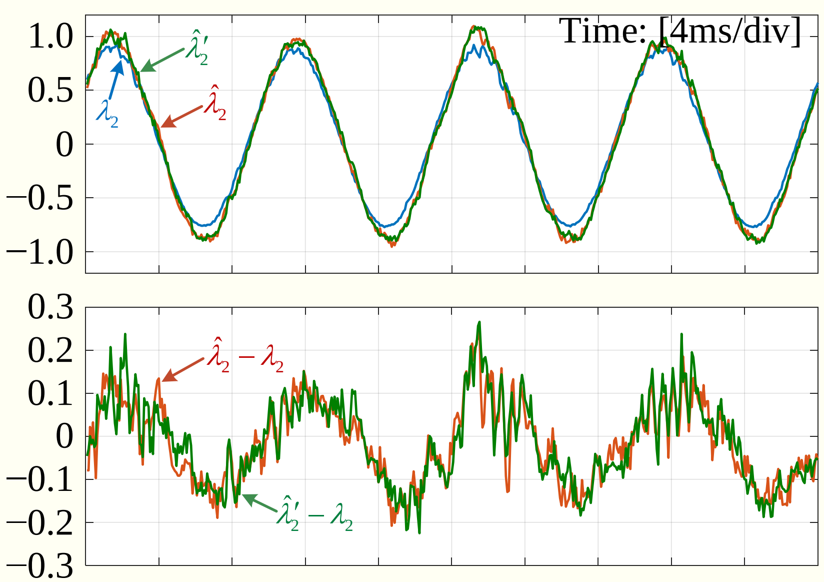

$\hat{\lambda}_3$ and $\hat{\lambda}_3'$ observers

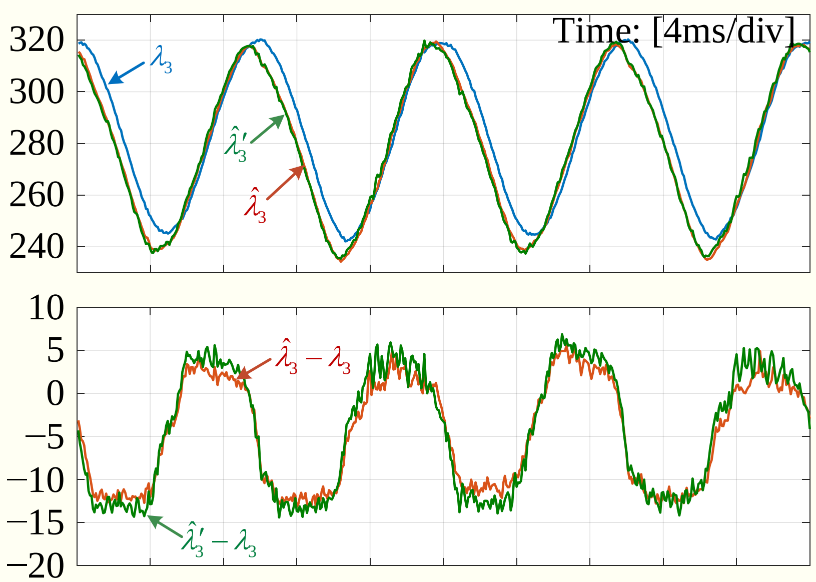

Experimental Verification

Comparison of the Computational Complexity

- The simplified algebraic observers achieve 95% reduction in the computational time.

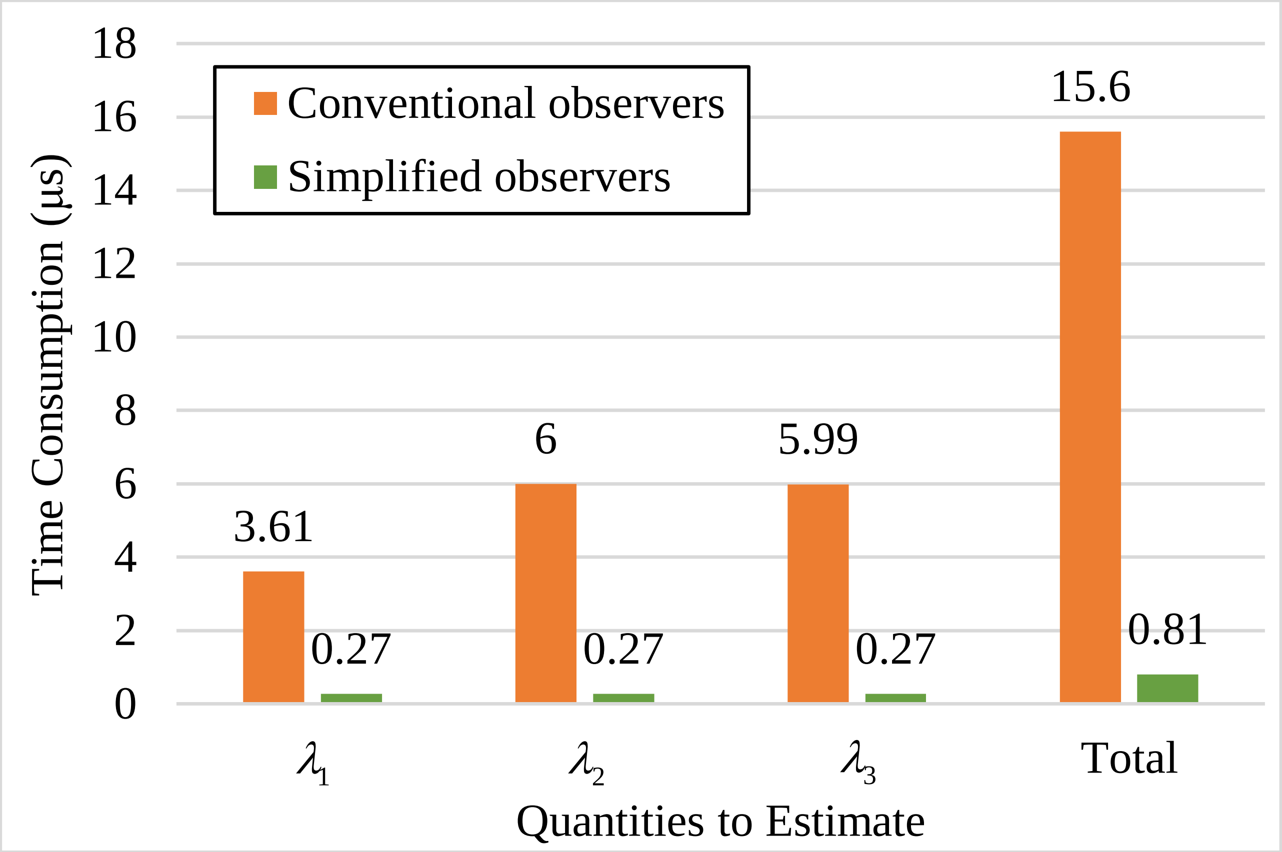

Experimental Verification

Performance of the Closed-Loop System

- **Experiment condition:** Steady-state operation (300 W).

- **AC port:**

  1) Unity power factor without the v_{ac} measurement;

  2) i_{ac} has a low THD of 2.02%.

- **DC port:**

  v_{dc} regulated at 400 V with a ripple of ±1%.

- **APPB port:**

  v_b has a large voltage swing of 70 V.

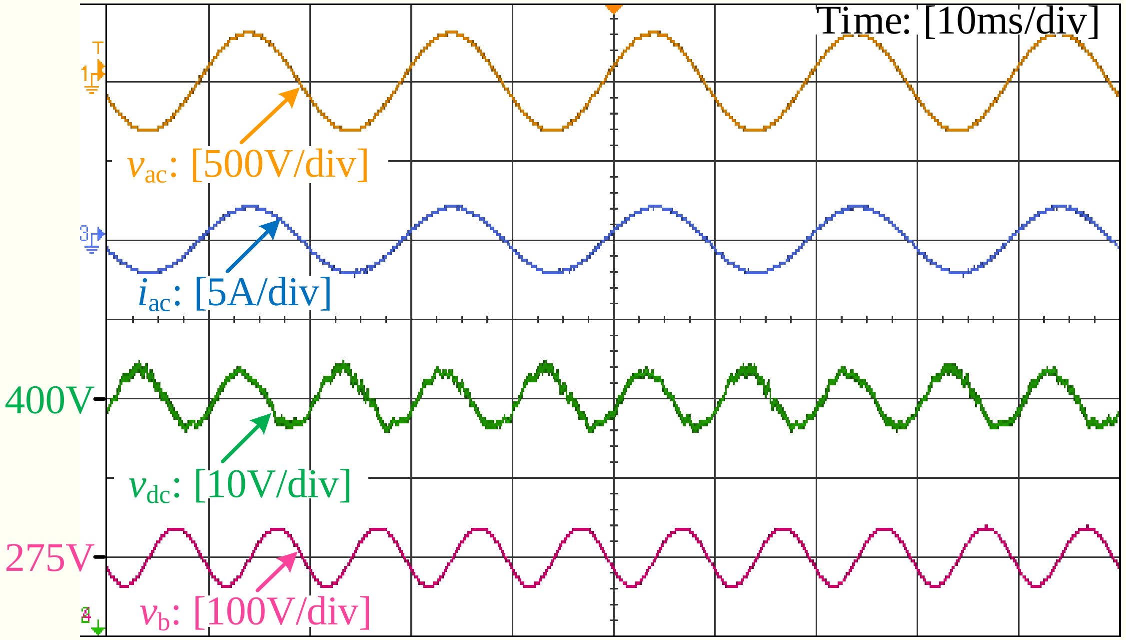

Experimental Verification

Performance of the Closed-Loop System

- **Experiment condition:**

  Load power change: 0 W → 300 W and 300 W → 0 W.

- v_{dc} remains tightly regulated in the range of (400 ± 5) V.

- i_{ac} enters its steady-state within three line cycles.

- The simplified-observer-based controller is robust against load disturbances.

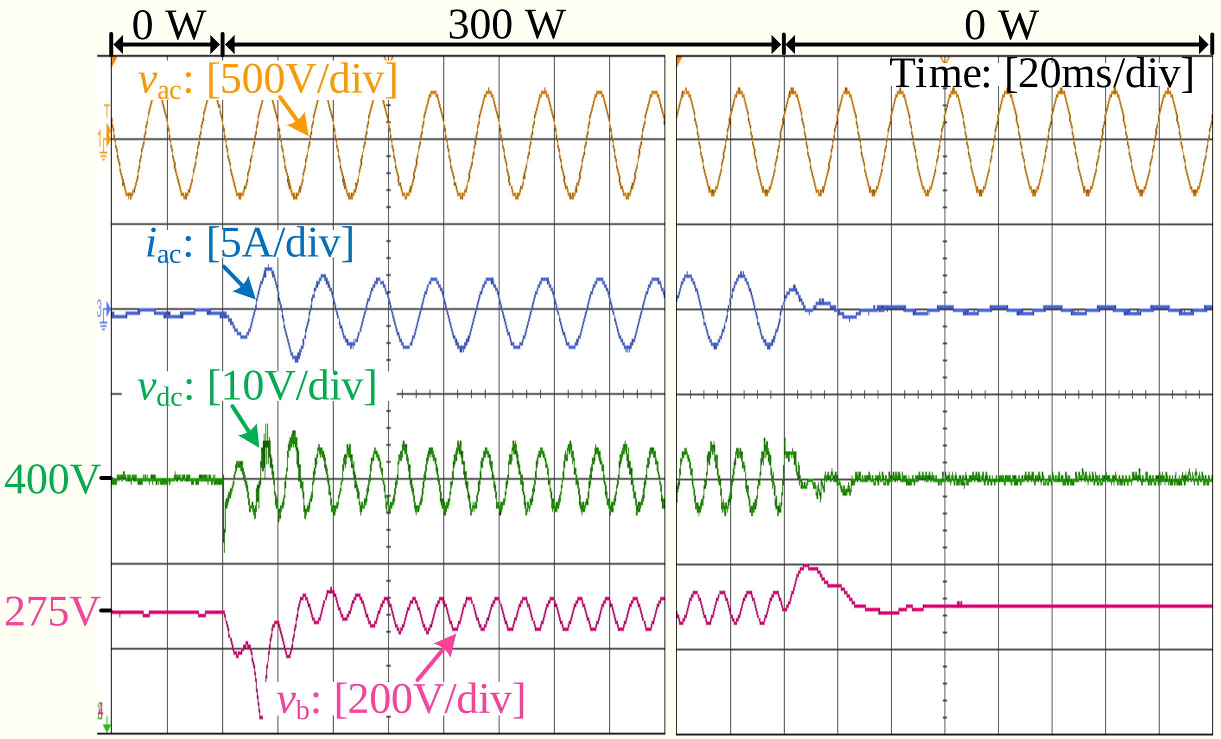

Experimental Verification

Performance of the Closed-Loop System

- **Experiment condition -** Reference of v_{dc}: 380 V → 420 V and 420 V → 380 V.
- v_{dc} has first-order responses with a settling time of 2 ms.
- The simple dynamics of the original controller are retained.

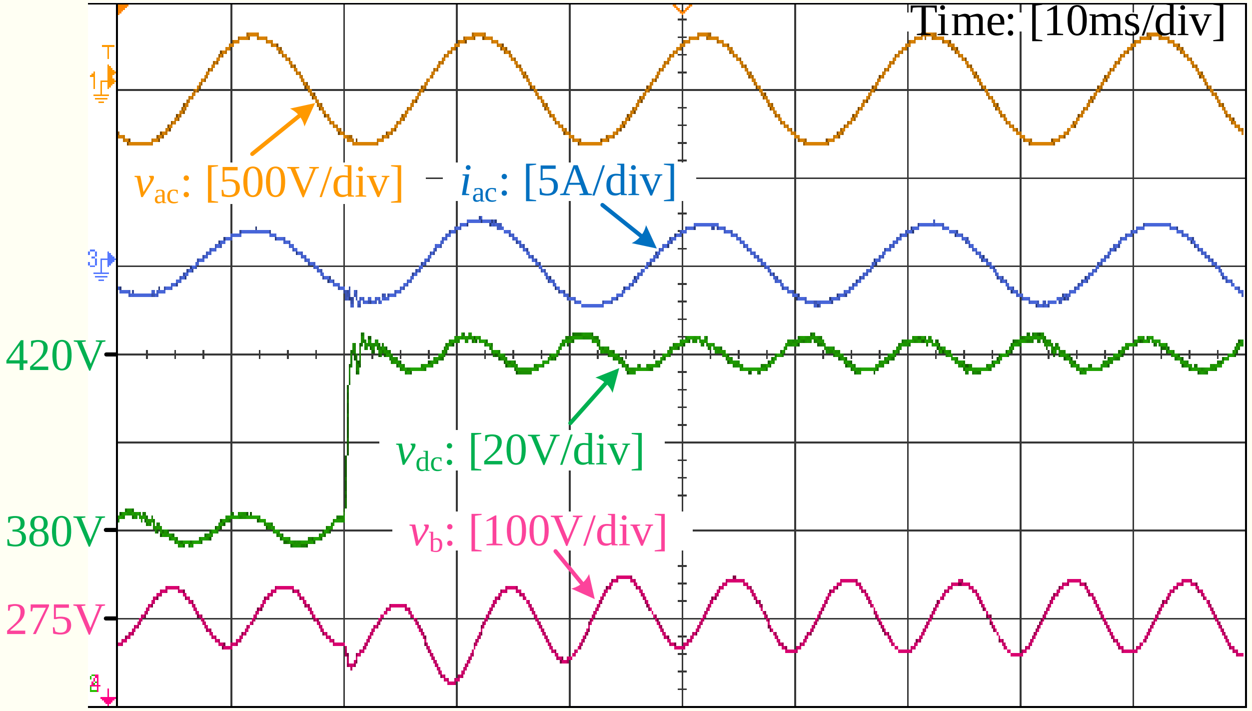

Outline

- Background of Single-Phase Converters with an APPB
- Review of Existing Control Methods
- Feedback-Linearization-Based APD Control
- Lyapunov-Based APD Control
- Sensor Count Reduction Using Algebraic Observers
- Sensor Count Reduction with Simplified Algebraic Observers
- Conclusions

Conclusions

- Based on the understanding of the characteristics of single-phase converters with an APPB, a systematic controller design method is discussed. The FLB-APD control is applicable when internal dynamics are stable, while the LB-APD control can be adopted when internal dynamics are unstable.

- Global stability, fast dynamics, and good robustness against disturbances are achieved with the FLB-APD and LB-APD control.

- To tackle the high-sensor-count problem, a sensor-reduction method based on algebraic observers is presented, which halves the number of sensors and retains the advantages of the original controller.

- A simplified algebraic observer is introduced, which reduces the computational time by 95% while achieving similar performance to that of the original algebraic observer.

Thanks for your attention!